PHYSICAL REVIEW D **83,** 074020 (2011)

One-Loop Helicity Amplitudes for $t\bar{t}$ Production at Hadron Colliders

Simon Badger*
The Niels Bohr International Academy and Discovery Center, The Niels Bohr Institute, Blegdamsvej 17, DK-2100 Copenhagen, Denmark

Ralf Sattler†
Institut für Physik, Humboldt-Universität zu Berlin, Newtonstraße 15, D-12489 Berlin, Germany and Deutsches Elektronen-Synchrotron DESY, Platanenallee 6, D-15738 Zeuthen, Germany

Valery Yundin‡
Institute of Physics, University of Silesia, Uniwersytecka 4, PL-40007 Katowice, Poland and Deutsches Elektronen-Synchrotron DESY, Platanenallee 6, D-15738 Zeuthen, Germany
(Received 8 March 2011; published 26 April 2011)

We present compact analytic expressions for all one-loop helicity amplitudes contributing to $t\bar{t}$ production at hadron colliders. Using recently developed generalized unitarity methods and a traditional Feynman based approach we produce a fast and flexible implementation.

DOI: 10.1103/PhysRevD.83.074020 PACS numbers: 12.38.Bx, 14.65.Ha

I. INTRODUCTION

The large production rate of top quarks at the Large Hadron Collider (LHC) [1], and the high numbers of leptonic decays, make it a key signal for the study of precision physics in the standard model (SM). The first theoretical predictions for the unpolarized cross section at next-to-leading order (NLO) have been known for over 20 years [2–5]. However, recent years have seen substantial progress in NLO predictions for heavy quark production and associated processes. Spin correlations and on shell decays of the top quarks at NLO [6,7] as well as electroweak corrections [8–14] are now well understood. One-loop amplitudes to higher order in the dimensional regularization parameter, which form part of the NNLO prediction, have also been computed [15,16]. Predictions for processes with heavy quark production in association with other QCD particles have also been made possible thanks to impressive calculations of $pp \to t\bar{t} + j$ [17–20], $pp \to t\bar{t}b\bar{b}$ [21–24] and $pp \to t\bar{t} + 2j$ [25]. Very recently, full off shell effects of the top decays have been computed [26,27].

The last few years have seen a rapid development in NLO techniques allowing the computation of new multileg amplitudes and cross sections. On shell techniques, which began with the development of the unitarity method [28,29], are quickly becoming an industry standard tool and, through working with gauge invariant building blocks, lead to extremely fast numerical evaluation for the virtual corrections to NLO processes [30–34]. Some of these methods have also been developed into public codes [35–37]. Together with advanced Feynman diagram based techniques many phenomenological predictions have been possible for $2 \to 4$ processes [21–27,38–43]. Last year also saw the first evaluations of $2 \to 5$ cross sections with computations of $pp \to W + 4j$ [44] and $e^+e^- \to 5j$ [45]. The extension of analytic unitarity techniques to deal with massive particles motivates the revisiting of the well-known process of heavy quark production in hadron collisions. In this paper we construct compact analytic expressions for the virtual helicity amplitudes. These amplitudes should lead to a flexible evaluation of the NLO cross section including both spin correlations and decays in the narrow width approximation. We demonstrate that the amplitudes presented here evaluate a factor of $\sim$10 times faster than the analytic results of Ref. [46] implemented in MCFM [47]. Full analytic computations also offer the possibility of investigating new structures in gauge theory amplitudes. In our particular example we find new simplicity in the subleading color contributions to the one-loop amplitudes.

Our paper is organized as follows. We first review the decomposition of the full one-loop amplitude into color ordered and primitive amplitudes which form the basic building blocks of our computation. We then give our notation for the spinor-helicity formalism used for the computation of helicity amplitudes with massive particles. In Sec. IV we outline the unitarity and Feynman based methods employed to arrive at the compact expression. We give details of the pole structures and renormalization procedure in Sec. V and VI before presenting the complete set of independent helicity amplitudes in Sec. VII and VIII. Some details of the numerical implementation are given in Sec. IX before we reach our conclusions. An Appendix listing the complete set of tree level amplitudes is included for completeness.

*simon.badger@nbi.dk
†ralf.sattler@physik.hu-berlin.de
‡valery.yundin@desy.de

II. COLOUR ORDERING AND PRIMITIVE AMPLITUDES

We follow the color decomposition into primitive amplitudes as described by Bern, Dixon and Kosower [48]. The case of massive quarks is identical to that of the massless case. Although we will talk of the processes $gg \to t\bar{t}$ and $q\bar{q} \to t\bar{t}$ throughout the paper, it should be noted that the amplitudes are computed with all particles considered to be outgoing.

A. The $gg \to t\bar{t}$ channel

First, the tree level amplitude can be written as

$$\mathcal{A}_4^{(0)}(1_t, 2, 3, 4_{\bar{t}}) = g_s^2 \sum_{P(2,3)} (T^{a_2}T^{a_3})_{i_1}^{\bar{t}_4} A_4^{(0)}(1_t, 2, 3, 4_{\bar{t}}), \quad (1)$$

while the one-loop amplitude reads

$$\mathcal{A}_4^{(1)}(1_t, 2, 3, 4_{\bar{t}}) = g_s^2 c_\Gamma \Bigg(\sum_{P(2,3)} N_c (T^{a_2}T^{a_3})_{i_1}^{\bar{t}_4} A_{4;1}^{(1)}(1_t, 2, 3, 4_{\bar{t}}) + \mathrm{tr}(T^{a_2}T^{a_3}) \delta_{i_1}^{\bar{t}_4} A_{4;3}^{(1)}(1_t, 4_{\bar{t}}; 2, 3) \Bigg), \quad (2)$$

where, in $D = 4 - 2\epsilon$ dimensions, c_Γ is defined as

$$c_\Gamma = \frac{\Gamma(1+\epsilon)\Gamma^2(1-\epsilon)}{(4\pi)^{2-\epsilon}\Gamma(1-2\epsilon)}. \quad (3)$$

The one-loop amplitudes can be further decomposed into gauge invariant primitive amplitudes:

$$A_{4;1}^{(1)}(1_t, 2, 3, 4_{\bar{t}}) = A_4^{[L]}(1_t, 2, 3, 4_{\bar{t}}) - \frac{1}{N_c^2} A_4^{[R]}(1_t, 2, 3, 4_{\bar{t}}) - \frac{N_f}{N_c} A_4^{[f]}(1_t, 2, 3, 4_{\bar{t}}) - \frac{N_H}{N_c} A_4^{[H]}(1_t, 2, 3, 4_{\bar{t}}), \quad (4)$$

$$A_{4;3}^{(1)}(1_t, 4_{\bar{t}}; 2, 3) = \sum_{P(2,3)} \Big\{ A_4^{[L]}(1_t, 2, 3, 4_{\bar{t}}) + A_4^{[L]}(1_t, 2, 4_{\bar{t}}, 3) + A_4^{[R]}(1_t, 2, 3, 4_{\bar{t}}) \Big\}, \quad (5)$$

where N_c is the number of colors, N_f and N_H are the number of light and heavy flavours, respectively. Explicitly the permutation set is $P(2, 3) = \{(2, 3), (3, 2)\}$.

Performing the color summations for the squared tree level amplitudes yields

$$\sum_{\mathrm{col}} |A_4^{(0)}|^2 = g_s^4 N_c (N_c^2 - 1) \sum_{P(2,3)} |A_4^{(0)}(1_t, 2, 3, 4_{\bar{t}})|^2 - \frac{N_c^2 - 1}{N_c} \Big| \sum_{P(2,3)} A_4^{(0)}(1_t, 2, 3, 4_{\bar{t}}) \Big|^2 \quad (6)$$

$$= g_s^4 N_c (N_c^2 - 1) \sum_{P(2,3)} |A_4^{(0)}(1_t, 2, 3, 4_{\bar{t}})|^2 - \frac{N_c^2 - 1}{N_c} |A_4^{(0)}(1_t, 2_\gamma, 3_\gamma, 4_{\bar{t}})|^2. \quad (7)$$

For the interference between the tree and one-loop amplitudes we find

$$\sum_{\mathrm{col}} \mathcal{A}_4^{(1)} [\mathcal{A}_4^{(0)}]^* = g_s^6 c_\Gamma N_c^2 (N_c^2 - 1) \sum_{P(2,3)} A_{4;1}^{(1)}(1_t, 2, 3, 4_{\bar{t}}) [A_4^{(0)}(1_t, 2, 3, 4_{\bar{t}})]^* + (N_c^2 - 1)(A_{4;3}^{(1)}(1_t, 4_{\bar{t}}; 2, 3) - A_{4;1}^{(1)}(1_t, 2, 3, 4_{\bar{t}}) - A_{4;1}^{(1)}(1_t, 3, 2, 4_{\bar{t}})) [A_4^{(0)}(1_t, 2_\gamma, 3_\gamma, 4_{\bar{t}})]^*. \quad (8)$$

B. The $q\bar{q} \to t\bar{t}$ channel

This time the tree level amplitude is

$$\mathcal{A}_4^{(0)}(1_t, 2_{\bar{q}}, 3_q, 4_{\bar{t}},) = g_s^2 \Big(\delta_{i_1}^{\bar{t}_2} \delta_{i_3}^{\bar{t}_4} - \frac{1}{N_c} \delta_{i_1}^{\bar{t}_4} \delta_{i_3}^{\bar{t}_2} \Big) A_4^{(0)}(1_t, 2_{\bar{q}}, 3_q, 4_{\bar{t}}), \quad (9)$$

while for the decomposition of the one-loop amplitude we find

$$\mathcal{A}_4^{(1)}(1_t, 2_{\bar{q}}, 3_q, 4_{\bar{t}}) = g_s^4 c_\Gamma (N_c \delta_{i_1}^{\bar{t}_2} \delta_{i_3}^{\bar{t}_4} A_{4;1}^{(1)}(1_t, 2_{\bar{q}}, 3_q, 4_{\bar{t}}) + \delta_{i_1}^{\bar{t}_4} \delta_{i_3}^{\bar{t}_2} A_{4;2}^{(1)}(1_t, 2_{\bar{q}}, 3_q, 4_{\bar{t}})), \quad (10)$$

with the primitives

$$A_{4;1}^{(1)}(1_t, 2_{\bar{q}}, 3_q, 4_{\bar{t}}) = A_4^{[lc]}(1_t, 2_{\bar{q}}, 3_q, 4_{\bar{t}}) - \frac{N_f}{N_c} A_4^{[f]}(1_t, 2_{\bar{q}}, 3_q, 4_{\bar{t}}) - \frac{N_H}{N_c} A_4^{[H]}(1_t, 2_{\bar{q}}, 3_q, 4_{\bar{t}}) - \frac{2}{N_c^2} (A_4^{[lc]}(1_t, 2_{\bar{q}}, 3_q, 4_{\bar{t}}) + A_4^{[lc]}(1_t, 3_q, 2_{\bar{q}}, 4_{\bar{t}})) - \frac{1}{N_c^2} A_4^{[slc]}(1_t, 2_{\bar{q}}, 3_q, 4_{\bar{t}}) \quad (11)$$

and

$$A_{4;2}^{(1)}(1_t, 2_{\bar{q}}, 3_q, 4_{\bar{t}}) = A_4^{[lc]}(1_t, 3_q, 2_{\bar{q}}, 4_{\bar{t}}) - \frac{N_f}{N_c} A_4^{[f]}(1_t, 3_q, 2_{\bar{q}}, 4_{\bar{t}}) - \frac{N_H}{N_c} A_4^{[H]}(1_t, 3_q, 2_{\bar{q}}, 4_{\bar{t}}) + \frac{1}{N_c^2} (A_4^{[lc]}(1_t, 3_q, 2_{\bar{q}}, 4_{\bar{t}}) + A_4^{[lc]}(1_t, 2_{\bar{q}}, 3_q, 4_{\bar{t}})) + \frac{1}{N_c^2} A_4^{[slc]}(1_t, 3_q, 2_{\bar{q}}, 4_{\bar{t}}). \quad (12)$$

Evaluating the color ordered squared tree level amplitude then yields

$$\sum_{\text{col}} |\mathcal{A}_4^{(0)}| = g_s^4 (N_c^2 - 1) |A_4^{(0)}(1_t, 2_{\bar{q}}, 3_q, 4_{\bar{t}})|^2, \tag{13}$$

whereas the interference term becomes

$$\sum_{\text{col}} \mathcal{A}_4^{(1)} [\mathcal{A}_4^{(0)}]^* = g_s^6 c_\Gamma N_c (N_c^2 - 1) A_{4;1}^{(1)}(1_t, 2_{\bar{q}}, 3_q, 4_{\bar{t}}) \times [A_4^{(0)}(1_t, 2_{\bar{q}}, 3_q, 4_{\bar{t}})]^*. \tag{14}$$

III. SPINOR-HELICITY FORMALISM

For massless particles it is possible to completely decompose all momenta into a basis of two component Weyl spinors since

$$p^\mu = \frac{1}{2} \langle p | \gamma^\mu | p]. \tag{15}$$

The polarization vectors and fermion wave functions then fit easily into a helicity basis:

$$u_+(p) = |p\rangle, \qquad u_-(p) = |p], \tag{16}$$

$$\epsilon_+^\mu(p, \xi) = \frac{\langle \xi | \gamma^\mu | p]}{\sqrt{2} \langle \xi p \rangle}, \qquad \epsilon_-^\mu(p, \xi) = \frac{\langle p | \gamma^\mu | \xi]}{\sqrt{2} [p \xi]}. \tag{17}$$

The situation for massive momenta is a little more complicated since (15) is no longer valid and the definition of a unique helicity state is no longer possible as one can always find a boost, through the rest frame, such that the helicity state is flipped. However, given a massive momentum, P, one can construct a helicity basis by defining a specific reference frame with respect to an arbitrary massless vector η [49]:

$$P^\mu = \alpha P^\flat + \beta \eta_P \tag{18}$$

where $\alpha\beta = \frac{m^2}{\langle P^\flat \eta_P \rangle [\eta_P P^\flat]}$. The u and v spinors can then be defined by

$$\begin{aligned} u_\pm(P, m; P^\flat, \eta_P) &= \frac{(P + m) | \eta_P \pm \rangle}{\sqrt{\alpha} \langle P^\flat \mp | \eta_P \pm \rangle}, \\ \bar{u}_\pm(P, m; P^\flat, \eta_P) &= \frac{\langle \eta_P \mp | (P + m)}{\sqrt{\alpha} \langle \eta_P \mp | P^\flat \pm \rangle}, \end{aligned} \tag{19}$$

$$\begin{aligned} v_\pm(P, m; P^\flat, \eta_P) &= \frac{(P - m) | \eta_P \pm \rangle}{\sqrt{\alpha} \langle P^\flat \mp | \eta_P \pm \rangle}, \\ \bar{v}_\pm(P, m; P^\flat, \eta_P) &= \frac{\langle \eta_P \mp | (P - m)}{\sqrt{\alpha} \langle \eta_P \mp | P^\flat \pm \rangle}. \end{aligned} \tag{20}$$

In the following we will set $\alpha = 1$ and $\beta = \frac{m^2}{2P^\flat \cdot \eta_P}$, which corresponds to the choice of Ref. [50] although a choice of

$$\begin{aligned} \alpha &= \frac{1}{2} \left(1 + \sqrt{1 - \frac{4m^2}{2P^\flat \cdot \eta_P}} \right), \\ \beta &= \frac{1}{2} \left(1 - \sqrt{1 - \frac{4m^2}{2P^\flat \cdot \eta_P}} \right) \end{aligned} \tag{21}$$

corresponds to the basis used in Ref. [51,52] which also has a convenient massless limit. A specific choice of the reference vector that allows us to match the four component representation of Ref. [19] is presented in Appendix B. Keeping the reference vectors η arbitrary allows us to relate the heavy quark helicity states:

$$u_-(P, m; P^\flat, \eta_P) = -\frac{\langle P^\flat \eta_P \rangle}{m} u_+(P, m; \eta_P, P^\flat), \tag{22}$$

$$v_-(P, m; P^\flat, \eta_P) = \frac{\langle P^\flat \eta_P \rangle}{m} v_+(P, m; \eta_P, P^\flat). \tag{23}$$

The spinor-helicity formalism is well suited for numerical evaluation and had been implemented for mathematica within the S@M package [53].

IV. METHODS

Each of our primitive one-loop amplitudes can be written using the standard basis of scalar integral functions and a rational term up to higher order terms in the dimensional regularization parameter ϵ:

$$\begin{aligned} A_4^{[X]}(1, 2, 3, 4) = {} & C_{4;1|2|3|4}^{[X]} I_{4;1|2|3|4}^{[X]} + \sum_{i=1}^{2} \sum_{j=i+1}^{3} \sum_{k=j+1}^{i-1} C_{3;i\ldots j-1|j\ldots k-1|k\ldots i-1}^{[X]} I_{3;i\ldots j-1|j\ldots k-1|k\ldots i-1}^{[X]} \\ & + \sum_{i=1}^{3} \sum_{j=i+1}^{i-1} C_{2;i\ldots j-1|j\ldots i-1}^{[X]} I_{2;i\ldots j-1|j\ldots i-1}^{[X]} + C_1^{[X]} I_1^{[X]} + R^{[X]} + \mathcal{O}(\epsilon). \end{aligned} \tag{24}$$

The indices $\{i, j, k, l\}$ denote the momenta at the external legs of the integrals and the sums run over all cyclic partitions. The dependence of the coefficients and the rational term on the helicity states of the external particles has been suppressed above. Figures 1–5 show the explicit basis integrals for the five independent primitive amplitudes. Heavy and light flavor fermion loop contributions have also been included.

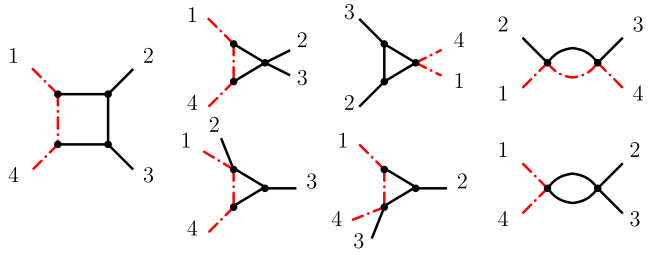

FIG. 1 (color online). The 7 cut diagrams contributing to the left-moving primitive amplitude in $gg \to t\bar{t}$. Red dotted lines represent massive fermions, plain lines represent gluons.

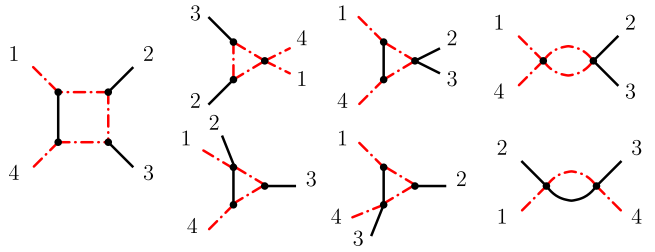

FIG. 2 (color online). The 7 cut diagrams contributing to the right-moving primitive amplitude in $gg \to t\bar{t}$. Red dotted lines represent massive fermions, plain lines represent gluons.

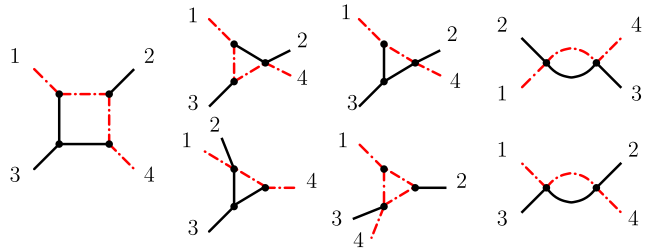

FIG. 3 (color online). The 7 cut diagrams contributing to the subleading color primitive amplitude in $gg \to t\bar{t}$. Red dotted lines represent massive fermions, plain lines represent gluons amplitude.

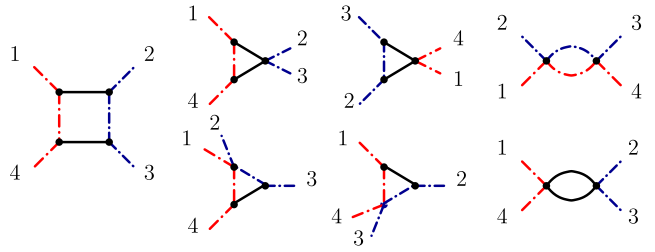

FIG. 4 (color online). The 7 cut diagrams contributing to the leading color primitive amplitude in $q\bar{q} \to t\bar{t}$. Red dotted lines represent massive fermions, plain lines represent gluons and blue dotted lines represent massless fermions.

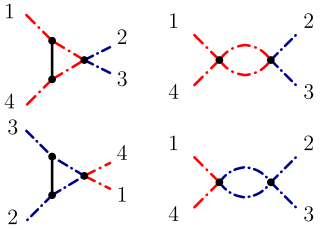

FIG. 5 (color online). The 4 cut diagrams contributing to the sub-leading color primitive amplitude in $q\bar{q} \to t\bar{t}$. Red dotted lines represent massive fermions, plain lines represent gluons and blue dotted lines represent massless fermions.

The computation was performed in two distinct parts. The first used generalized unitarity to compute the compact expressions for the coefficients of the scalar integrals. A Feynman diagram based approach was then taken to obtain compact forms for the remaining tadpoles and rational terms.

The computation was performed in the Four-Dimensional-Helicity (FDH) scheme and mass renormalization was performed using the on shell scheme.

A. Generalized unitarity

The use of the generalized unitarity [32,54–58], extended to massive propagators [19,59–61], is the primary reason we are able to obtain compact representations for the one-loop helicity amplitudes. The analytic techniques we have employed are by now well covered in the existing literature and have been used extensively in recent analytic computations of $pp \to H + 2j$ [62–64] and $pp \to Wb\bar{b}$ [65] production. We refer the reader to recent reviews on the topic for further details [66,67]. However, since analytic computations for massive amplitudes are covered to a lesser extent, we outline some of the techniques specific to our process.

D-dimensional cutting procedures [32,59,68,69] could also be applied to the computation of rational terms in massive amplitudes as described in Ref. [19]. However, as we discuss briefly in Sec. IV A 3, the procedure can lead to large intermediate expressions when followed analytically. On shell recursion relations offer an attractive alternative to obtain compact expressions directly [70–73]. At the present time such techniques have yet to be extended to the massive case. A Feynman diagram approach therefore offers a simple way to obtain compact analytic expressions for our process.

1. Three-Mass triangle Coefficients

In this section we give an explicit example of the computation for the three-(external)-mass triangle coefficient $C_{3;1|23|4}$. This gives a good example of a computation that is specific to the massive case. We consider the $++-+$ helicity configuration in the $gg \to t\bar{t}$ since the $++++$ configuration is zero. Following Forde's method [57], the

triple cut can be parametrized by a one-dimensional complex contour integral over t. The on shell constraints for the loop momentum are solved in general leaving the integrand as a rational function of t. The scalar triangle coefficient is then given as the boundary value of this triple cut integrand:

$$C^{[L]}_{3;4|1|23}(1_t^+, 2^+, 3^-, 4_{\bar{t}}^+) = -\frac{1}{2}\sum_{\gamma_\pm} \inf_t [\tilde{C}^{[L]}_{3;4|1|23}(1_t^+, 2^+, 3^-, 4_{\bar{t}}^+)]|_{t^0}, \quad (25)$$

$$\tilde{C}^{[L]}_{3;4|1|23}(1_t^+, 2^+, 3^-, 4_{\bar{t}}^+) = \sum_{h_1=\pm}\sum_{h_2=\pm}\sum_{h_3=\pm} A^{(0)}(-l_3^{-h_3}, 4_{\bar{t}}^+, l_{1;t}^{h_1}) \times A^{(0)}(-l_{1;\bar{t}}^{-h_1}, 1_t^+, l_2^{h_2}) A^{(0)}(-l_2^{-h_2}, 2^+, 3^-, l_3^{h_3}), \quad (26)$$

where $\inf_t$ is computed by taking a Taylor expansion around $t = \infty$. The complex parameter t appears in the parametrization of the (on shell) loop momentum. We construct a spinor basis for the complex loop momentum using two massless vectors $K_1^\flat$ and $K_2^\flat$. In our case the massless vectors can be constructed from p_4 and p_1 such that

$$K_1^{\flat,\mu} = \frac{\gamma(\gamma p_4^\mu - m^2 p_1^\mu)}{\gamma^2 - m^4}, \quad (27)$$

$$K_2^{\flat,\mu} = \frac{\gamma(\gamma p_1^\mu - m^2 p_4^\mu)}{\gamma^2 - m^4}, \quad (28)$$

where $\gamma_\pm = p_1 \cdot p_4 \pm \sqrt{(p_1 \cdot p_4)^2 - m^4}$. The on shell loop momentum l_1 can then be written as

$$l_1^\mu = a(K_1^{\flat,\mu} - K_2^{\flat,\mu}) + \frac{t}{2}\langle K_1^\flat|\gamma^\mu|K_2^\flat] - \frac{a^2\gamma + m^2}{2\gamma t}\langle K_2^\flat|\gamma^\mu|K_1^\flat], \quad (29)$$

where

$$a = \frac{m^2}{\gamma - m^2}. \quad (30)$$

The procedure from this point is rather straightforward. For illustrative purposes we find it convenient to expand the helicity sum in Eq. (26) and explicitly remove dependence of the internal reference vector of the massive spinor. This results in considerably shorter expressions for the integrand, though in general we find that specific choices of this vector yield comparable sized expressions after expansion. Inserting the relevant tree amplitudes from Appendix A we find (the reference vectors for the internal gluons were chosen as $\xi^\mu_{l_2} = \xi^\mu_{l_3} = \frac{1}{2}\langle K_2^\flat|\gamma^\mu|K_1^\flat]$)

$$-i\tilde{C}^{[L]}_{3;4|1|23}(1_t^+, 2^+, 3^-, 4_{\bar{t}}^+) = \frac{m\langle K_2^\flat|1|l_2]\langle\langle\eta_4\eta_1\rangle\langle l_3|4|K_1^\flat] + \langle l_3\eta_1\rangle\langle l_3\eta_4\rangle[K_1^\flat l_3]\rangle\langle l_2 3\rangle^4}{\langle\eta_4 4^\flat\rangle\langle K_2^\flat l_2\rangle\langle l_2 l_3\rangle\langle l_2 2\rangle\langle l_3 3\rangle\langle 1^\flat\eta_1\rangle\langle 23\rangle[K_1^\flat l_3]} + \frac{m\langle l_3 3\rangle_2^3\langle K_2^\flat|4|l_3]\langle\langle\eta_4\eta_1\rangle\langle l_2|1|K_1^\flat] + \langle l_2\eta_1\rangle\langle l_2\eta_4\rangle[K_1^\flat l_2]\rangle}{\langle\eta_4 4^\flat\rangle\langle K_2^\flat l_3\rangle\langle l_2 l_3\rangle\langle l_2 2\rangle\langle 1^\flat\eta_1\rangle\langle 23\rangle[K_1^\flat l_2]}. \quad (31)$$

We are then left to feed in the parametrization of (29), expand around $t = \infty$ and extract the coefficient of t^0. This analytic form still contains the dependence on $\gamma_\pm$ and we must still perform the sum before we arrive at the full scalar triangle coefficient. In principle this can be done numerically but in this case we find the analytic form after the t expansion is rather lengthy and we can improve the situation considerably by performing the sum analytically. The procedure is straightforward but tends to lead us through relatively large intermediate expressions. We begin by removing all ''flatted'' spinors in place of an explicit polynomial in γ. To do this, we make sure not to introduce spurious denominators by making use of

$$\langle 2|K_1^\flat|3] = -\frac{\gamma}{\gamma - m^2}\langle 2|1|3]. \quad (32)$$

The sum of the two solutions $\gamma_\pm$ is obtained from this polynomial form by rearrangement into a function of

$$\gamma_+ + \gamma_- = 2p_1 \cdot p_4, \qquad \gamma_+\gamma_- = m^4. \quad (33)$$

We are then left to partial fraction the spinor products. After the dust clears, we are left with a relatively compact form:

$$
\begin{aligned}
&iC^{[L]}_{3;4|1|23}(1_t^+, 2^+, 3^-, 4_{\tilde{t}}^+) \\
&= \frac{6(\langle\eta_4\eta_1\rangle\langle 23\rangle - 2\langle 2\eta_4\rangle\langle 3\eta_1\rangle)\langle 3|1|2]^2 m^3}{\beta^4 s_{23}^2\langle\eta_1 1^\flat\rangle\langle\eta_4 4^\flat\rangle\langle 23\rangle} + \frac{2(\langle 2\eta_4\rangle\langle 3\eta_1\rangle - \langle\eta_4\eta_1\rangle\langle 23\rangle)(s_{23} + 2\langle 2|1|2])\langle 3|1|2]m^3}{\beta^2 s_{23}\langle\eta_1 1^\flat\rangle\langle\eta_4 4^\flat\rangle\langle 23\rangle\langle 2|1|3]} \\
&\quad - \frac{2(2m^2 + \langle 2|1|2])\langle 2\eta_1\rangle\langle 2\eta_4\rangle\langle 3|1|2]m^3}{\beta^2\langle\eta_1 1^\flat\rangle\langle\eta_4 4^\flat\rangle\langle 23\rangle\langle 2|1|3]^2} + \frac{(s_{23} + 2\langle 2|1|2])\langle 2\eta_1\rangle\langle 3\eta_4\rangle[32]m^3}{\langle\eta_1 1^\flat\rangle\langle\eta_4 4^\flat\rangle\langle 2|1|3]^2} + \frac{\langle 2\eta_1\rangle\langle 2\eta_4\rangle\langle 3|1|2]^2 m}{2\langle\eta_1 1^\flat\rangle\langle\eta_4 4^\flat\rangle\langle 23\rangle\langle 2|1|3]} \\
&\quad - \frac{\langle 3\eta_1\rangle\langle 3\eta_4\rangle\langle 3|1|2]m}{2\langle\eta_1 1^\flat\rangle\langle\eta_4 4^\flat\rangle\langle 23\rangle} + \frac{s_{12}\langle\eta_4\eta_1\rangle\langle 3|1|2]m}{\langle\eta_1 1^\flat\rangle\langle\eta_4 4^\flat\rangle\langle 2|1|3]} - \frac{(\langle 3\eta_1\rangle\langle 3\eta_4\rangle\langle 2|1|3] - \langle 2\eta_1\rangle\langle 2\eta_4\rangle\langle 3|1|2])\langle 3|1|2]m}{4\beta^2\langle\eta_1 1^\flat\rangle\langle\eta_4 4^\flat\rangle\langle 23\rangle\langle 2|1|3]} \\
&\quad + \frac{3(8\langle 2|1|2]m^2 + s_{23}^2)(\langle 3\eta_1\rangle\langle 3\eta_4\rangle\langle 2|1|3] - \langle 2\eta_1\rangle\langle 2\eta_4\rangle\langle 3|1|2])\langle 3|1|2]m}{4\beta^4 s_{23}^2\langle\eta_1 1^\flat\rangle\langle\eta_4 4^\flat\rangle\langle 23\rangle\langle 2|1|3]} + \frac{\langle 2\eta_1\rangle\langle 2\eta_4\rangle\langle 2|1|2]\langle 3|1|2][32]m}{2\langle\eta_1 1^\flat\rangle\langle\eta_4 4^\flat\rangle\langle 2|1|3]^2} \\
&\quad + \frac{(2m^2 + \langle 3|1|3])\langle 3\eta_1\rangle\langle 3\eta_4\rangle[32]m}{2\langle\eta_1 1^\flat\rangle\langle\eta_4 4^\flat\rangle\langle 2|1|3]} + \frac{(2m^2 + \langle 2|1|2])s_{23}\langle 2\eta_1\rangle\langle 2\eta_4\rangle\langle 2|1|2][32]m}{2\langle\eta_1 1^\flat\rangle\langle\eta_4 4^\flat\rangle\langle 2|1|3]^3} - \frac{\beta^2 s_{12}s_{23}^2\langle\eta_4\eta_1\rangle m}{2\langle\eta_1 1^\flat\rangle\langle\eta_4 4^\flat\rangle\langle 2|1|3]^2},
\end{aligned}
\tag{34}
$$

where $\beta = \sqrt{1 - \frac{4m^2}{s_{23}}}$. Although one may not consider this form particularly elegant we note that it is much shorter than expression before the γ sum. It is also among the most complicated coefficients that we encountered in the computation.

2. Bubble coefficients

In this section we apply the Taylor expansion method to the computation of the bubble coefficient $C^{[L]}_{2;12|34}(1_t^+, 2^+, 3^+, 4_{\tilde{t}}^+)$. The on shell constraints can be solved in general leaving two free complex parameters which we label t and y. Owing to the two dimensional complex integration the pole structure is rather more involved than the triple cut considered above and we must consider triple cut contributions as well as the double cut in order compute the full coefficient[1] Our coefficient can therefore be written as

$$
\begin{aligned}
C_{2;12;34}(1_t^+, 2^+, 3^+, 4_{\tilde{t}}^+) = &-i\inf_t[\inf_y[\tilde{C}_{2;12|34}(1_t^+, 2^+, 3^+, 4_{\tilde{t}}^+)]] - \frac{1}{2}\sum_{y_\pm}\inf_t[\tilde{C}_{3;12|3|4}(1_t^+, 2^+, 3^+, 4_{\tilde{t}}^+)]] \\
&- \frac{1}{2}\sum_{y_\pm}\inf_t[\tilde{C}_{3;1|2|34}(1_t^+, 2^+, 3^+, 4_{\tilde{t}}^+)]],
\end{aligned}
\tag{35}
$$

where we choose to parametrize the loop momentum as

$$
l_1^\mu = yK_1^\mu - \frac{\langle 2|1|2] - ys_{12}}{\langle 2|1|2]}p_3^\mu + \frac{t}{2}\langle K_1^\flat|\gamma^\mu|3] + \frac{y(\langle 2|1|2] - ys_{12})}{2t\langle 2|1|2]}\langle 3|\gamma^\mu|K_1^\flat] \tag{36}
$$

with $K_1^\flat = p_4 - \frac{m^2}{\langle 2|1|2]}p_3$. In fact, with this choice we find the second term above vanishes. This is particularly convenient analytically, however, for a direct numerical evaluation, an independent massless vector would yield more stable results. Using the compact expressions for the tree level amplitudes and summing over the internal helicities gives the integrands for the two nonzero contributions to be

$$
\tilde{C}_{2;12|34}(1_t^+, 2^+, 3^+, 4_{\tilde{t}}^+) = \frac{m^3([l_1 2]^2\langle l_1|4|3]^2 + [l_1 3]^2\langle l_1|1|2]^2)\langle\eta_1\eta_4\rangle}{\langle 2|1|2]^2\langle 13\rangle[l_1 2][l_1 3]\langle 2l_1\rangle\langle\eta_1 1^\flat\rangle\langle\eta_4 4^\flat\rangle} + \frac{m^3[23]\langle l_1\eta_1\rangle\langle l_1\eta_4\rangle}{\langle 2|1|2]\langle l_1 2\rangle\langle l_1 3\rangle\langle\eta_1 1^\flat\rangle\langle\eta_4 4^\flat\rangle}, \tag{37}
$$

and,

$$
\begin{aligned}
\tilde{C}_{3;1|2|34}(1_t^+, 2^+, 3^+, 4_{\tilde{t}}^+) = &\frac{im[l_1 2]^3\langle l_1|4|3]\langle 3|1 l_3|3\rangle([l_1 3]\langle l_1\eta_1\rangle\langle l_1\eta_4\rangle + \langle l_1|4|3]\langle\eta_1\eta_4\rangle)}{\langle 2|1|2][l_1 3]\langle l_1 3\rangle\langle 3|l_3|l_1]\langle\eta_1 1^\flat\rangle\langle\eta_4 4^\flat\rangle} \\
&- \frac{im^3\langle 3|1|2]^3[l_1 3]\langle l_1 2\rangle^2\langle\eta_1\eta_4\rangle}{\langle 2|1|2]\langle l_1 3\rangle\langle 2|l_3 4|3\rangle\langle 3|l_3 4|3\rangle\langle\eta_1 1^\flat\rangle\langle\eta_4 4^\flat\rangle} \\
&+ \frac{im^3[l_1 3](\langle\eta_1|l_3|2]\langle\eta_4|l_3|2] - [2|l_3 1|2]\langle\eta_1\eta_4\rangle)}{\langle 2|1|2][l_1 2]\langle l_1 3\rangle\langle 3|l_3|l_1]\langle\eta_1 1^\flat\rangle\langle\eta_4 4^\flat\rangle}.
\end{aligned}
\tag{38}
$$

[1]The alternative method of spinor integration produces an identical set of poles as can be seen from Mastrolia's evaluation of the double cut via Stoke's theorem [58].

Just as in the three-mass triangle, we find a considerable benefit from taking the extra effort to find a closed form for the triangle contributions which are free of square roots. Many terms cancel between the double and triple cuts so that the final result is simply

$$-iC^{[L]}_{2;12|34}(1_t^+, 2^+, 3^+, 4_{\bar{t}}^+) = \frac{m^3[32](\langle\eta_1|(1+2)(2+3)|\eta_4\rangle) - s_{12}m^2}{\langle 2|1|2]^2\langle\eta_1 1^\flat\rangle\langle\eta_4 4^\flat\rangle\langle 23\rangle}. \quad (39)$$

3. Tadpole and On Shell bubble coefficients

The computation of the tadpole coefficients directly from unitarity is complicated by the fact that the wave function renormalization contributions cause the double cuts to diverge. A way around this problem has been introduced in the context of a numerical application of D-dimensional generalized unitarity in Ref. [19]. The method should apply equally well to analytic evaluation, but since it breaks gauge invariance, it can lead to large intermediate expressions. Such cuts also require the six-point tree level amplitudes rendering the computation more difficult. Nevertheless, methods using spinor integration technique have been proposed [74,75].

Both the tadpole and on shell bubble coefficients combine to give the coefficient of the $\log(m^2)$ contribution to the full amplitude. The coefficient of this logarithm is completely fixed by the universal IR constraints once combined with the knowledge of the cuts considered in the previous section. With this in mind, we rearrange the integral basis as

$$A_4^{[X]}(1,2,3,4) = C^{[X]}_{4;1|2|3|4} I^{[X]}_{4;1|2|3|4} + \sum_{i=1}^{2}\sum_{j=i+1}^{3}\sum_{k=j+1}^{i-1} C^{[X]}_{3;i\ldots j-1|j\ldots k-1|k\ldots i-1} I^{[X]}_{3;i\ldots j-1|j\ldots k-1|k\ldots i-1} + \sum_{i=1}^{2}\sum_{j=i+2}^{i-2} C^{[X]}_{2;i\ldots j-1|j\ldots i-1} I^{[X]}_{2;i\ldots j-1|j\ldots i-1} + C^{[X]}_{2;m^2} I^{[X]}_{2;m^2} + R'^{[X]} + \mathcal{O}(\epsilon). \quad (40)$$

For the gluon fusion channel the universal poles structure implies

$$C^{[L]}_{2;m^2} = -C^{[L]}_{2;12|34} - C^{[L]}_{2;23|41} + \frac{1}{2}A_4^{(0)}, \quad (41)$$

$$C^{[R]}_{2;m^2} = -C^{[R]}_{2;12|34} - C^{[R]}_{2;23|41} + \frac{1}{2}A_4^{(0)}, \quad (42)$$

$$C^{[H]}_{2;m^2} = -C^{[H]}_{2;23|41} \quad (43)$$

and the quark annihilation channel,

$$C^{[lc]}_{2;m^2} = -C^{[lc]}_{2;12|34} - C^{[lc]}_{2;12|34} + \frac{8}{3}A_4^{(0)}, \quad (44)$$

$$C^{[slc]}_{2;m^2} = -C^{[slc,m]}_{2;23|41} - C^{[slc,0]}_{2;23|41} - A_4^{(0)}, \quad (45)$$

$$C^{[H]}_{2;m^2} = -C^{[H]}_{2;23|41} + \frac{2}{3}A_4^{(0)}. \quad (46)$$

In this case we returned to a Feynman based computation of the rational terms and remaining tadpole contributions. Owing to the simplified form of the reduction algorithm, and the fact that such contributions are independently gauge invariant, the approach gives a simple way to reach a compact form for the full amplitude. The final results for the tadpole coefficients turn out to be remarkably simple and suggest that an approach based on matching with the universal IR and UV structure, as proposed in Ref. [59,60], would generalize to all massive amplitudes. A complete description, however, remains for future study.

B. Feynman diagram based approach

To compute a rational contribution and provide numerical cross-checks for cut-constructible parts of the amplitude we have performed two independent calculations based on the traditional Feynman diagram approach.

The diagrams were generated with DIANA [76] and then further processed analytically with two independent FORM [77] codes, to generate tensor integral representations of the color ordered one-loop amplitude. The tensor integrals were reduced to scalar boxes, triangles and bubbles in $4-2\epsilon$ dimensions using standard Passarino-Veltman reduction in one case and to scalar integrals in shifted dimension according to [78–81] in the second case. We performed calculations using both Dirac-spinor and spinor-helicity methods in Four-Dimensional-Helicity (FDH) and 't Hooft-Veltman (HV) schemes, which allowed us to verify that scheme dependence is in agreement with predictions of [82].

To maintain amplitude invariance under gauge transformations of gluon fields it is necessary to perform finite renormalization of the heavy quark mass [19]. This is done by including mass counterterm diagrams with the mass renormalization defined by

$$m = (1 + \delta Z_m)m^R, \quad (47)$$

where

$$\delta Z_m = -g_s^2 c_\Gamma C_F\left(\frac{3}{\epsilon} + 3\log\left(\frac{\mu_R^2}{m^2}\right) + 5\right). \quad (48)$$

V. POLE STRUCTURE

We have verified that our amplitudes satisfy the well-known universal Infra-Red and Ultra-Violet pole structures [82]. These can be broken down into the contributions from each primitive amplitude [19]. Representing the divergent parts of the amplitude by the function $V^{[X]}$ we can write

$$A_4^{[X]} = V^{[X]} A_4^{(0)} + F^{[X]}. \tag{49}$$

For the gluon channel we find (β as defined after Eq. (34)):

$$V_4^{[L]}(1_t, 2, 3, 4_{\bar{t}}) = -\frac{2}{\epsilon^2} + \frac{1}{2\epsilon} - \frac{1}{\epsilon}\log\left(\frac{\mu_R^2 m^2}{\langle 2|1|2]^2}\right) - \frac{1}{\epsilon}\log\left(-\frac{\mu_R^2}{s_{23}}\right), \tag{50}$$

$$V_4^{[R]}(1_t, 2, 3, 4_{\bar{t}}) = \frac{1}{2\epsilon} - \frac{1}{\epsilon}\frac{s_{23} - 2m^2}{s_{23}\beta}\log\left(\frac{1-\beta}{1+\beta}\right). \tag{51}$$

For the subleading color we list the poles of the full color ordered amplitude which is proportional to $A_4^{(0)}(1_t, 2, 3, 4_{\bar{t}}) + A_4^{(0)}(1_t, 3, 2, 4_{\bar{t}}) = A_4^{(0)}(1_t, 2_\gamma, 3_\gamma, 4_{\bar{t}})$:

$$V^{[slc]}(1_t, 2, 3, 4_{\bar{t}}) = \frac{\langle 2|1|2]}{s_{23}\epsilon}\log\left(\frac{\mu_R^2 m^2}{\langle 2|1|2]^2}\right) + \frac{\langle 3|1|3]}{s_{23}\epsilon}\log\left(\frac{\mu_R^2 m^2}{\langle 3|1|3]^2}\right) + \frac{1}{\epsilon}\log\left(-\frac{\mu_R^2}{s_{23}}\right) + \frac{1}{\epsilon}\frac{s_{23} - 2m^2}{s_{23}\beta}\log\left(\frac{1-\beta}{1+\beta}\right). \tag{52}$$

The poles of full color and helicity summed interference with the tree level can be written in terms of spin correlated Born amplitudes:

$$2\sum_{c,h}\mathcal{A}^{(1)}\cdot[\mathcal{A}^{(0)}]^* = 2N_c\sum_{c,h}\left\{|\mathcal{A}^{(0)}(2,3)|^2 V^{[L]}(1_t, 2, 3, 4_{\bar{t}}) + |\mathcal{A}^{(0)}(3,2)|^2 V^{[L]}(1_t, 3, 2, 4_{\bar{t}}) - \frac{1}{N_c^2}|\mathcal{A}_4^{(0)}|^2 V^{[R]} - |\mathcal{A}_{4;\gamma}^{(0)}|^2 V^{[slc]}\right\}, \tag{53}$$

where

$$\sum_{c,h}|\mathcal{A}_4^{(0)}(2,3)|^2 = \frac{N_c^2 - 1}{N_c}\sum_h (N_c^2 - 1)|A_4^{(0)}(1_t, 2, 3, 4_{\bar{t}})|^2 + A_4^{(0)}(1_t, 2, 3, 4_{\bar{t}})[A_4^{(0)}(1_t, 3, 2, 4_{\bar{t}})]^*, \tag{54}$$

and $\sum_{c,h}|\mathcal{A}_4^{(0)}(2,3)|^2 + |\mathcal{A}_4^{(0)}(3,2)|^2 = \sum_{c,h}|\mathcal{A}_4^{(0)}|^2$. Turning our attention to the quark channel the analogous structure can be written as

$$V^{[lc]}(1_t, 2_{\bar{q}}, 3_q, 4_{\bar{t}}) = \frac{1}{\epsilon^2} + \frac{8}{3\epsilon} - \frac{1}{\epsilon}\log\left(\frac{\mu_R^2 m^2}{\langle 2|1|2]^2}\right), \tag{55}$$

$$V^{[slc]}(1_t, 2_{\bar{q}}, 3_q, 4_{\bar{t}}) = \frac{1}{\epsilon^2} - \frac{1}{\epsilon} - \frac{1}{\epsilon}\log\left(-\frac{\mu_R^2}{s_{23}}\right) - \frac{1}{\epsilon}\frac{s_{23} - 2m^2}{s_{23}\beta}\log\left(\frac{1-\beta}{1+\beta}\right), \tag{56}$$

$$V^{[f]}(1_t, 2_{\bar{q}}, 3_q, 4_{\bar{t}}) = V^{[f]}(1_t, 2_{\bar{q}}, 3_q, 4_{\bar{t}}) = \frac{2}{3\epsilon}, \tag{57}$$

$$2\sum_{c,h}\mathcal{A}_4^{(1)}\cdot[\mathcal{A}_4^{(0)}]^* = 2\sum_{c,h}|\mathcal{A}_4^{(0)}|^2\left\{N_c V^{[lc]}(1_t, 2_{\bar{q}}, 3_q, 4_{\bar{t}}) - (N_f + N_H)V^{[f]} - \frac{2}{N_c}(V^{[lc]}(1_t, 2_{\bar{q}}, 3_q, 4_{\bar{t}}) - V^{[lc]}(1_t, 3_{\bar{q}}, 2_q, 4_{\bar{t}})) - \frac{1}{N_c}V^{[slc]}(1_t, 2_{\bar{q}}, 3_q, 4_{\bar{t}})\right\}. \tag{58}$$

VI. RENORMALIZATION AND SCHEME DEPENDENCE

The one-loop amplitudes presented in the previous sections still contain UV divergences which need to be renormalized. At this point we want to remind the reader that we already included the mass renormalization for the top quark mass, which we define using the pole scheme. Thus we are left with the wave function renormalization and the running of the strong coupling constant. For the former we are using an on shell prescription which takes into account all self energy contributions, whereas the coupling constant is renormalized in the $\overline{\text{MS}}$ scheme. To decouple the top quark from the running of α_s, one subtracts the diagrams with a top quark in the loop at zero momentum transfer. Following [83,84] we define the renormalization constants for the gluon and fermion fields and that of the strong coupling:

$$\begin{aligned} G_{a,\mu}^0 &= (1 + \delta Z_G/2)G_{a,\mu}, \\ \psi_Q^0 &= (1 + \delta Z_Q/2)\psi_Q, \\ (g_s^0)^2 &= (1 + \delta Z_{g_s})g_s^2, \end{aligned} \tag{59}$$

where, in the FDH scheme,

$$\delta Z_Q = \delta Z_m, \qquad \delta Z_G = -\frac{2g_s^2 c_\Gamma}{3\epsilon}\left(\frac{\mu_R^2}{m^2}\right)^\epsilon, \tag{60}$$

$$\delta Z_{g_s} = -g_s^2 c_\Gamma\left\{\frac{1}{\epsilon}\left(\frac{11}{3}N_c - \frac{2}{3}N_f - \frac{2}{3}\left(\frac{\mu_R^2}{m^2}\right)^\epsilon\right) - \frac{N_c}{3}\right\}, \tag{61}$$

with $C_F = \frac{N_c^2-1}{2N_c}$. Details of the scheme dependence of the coupling constant renormalization can be found in Ref. [85]. Summing up all contributions the renormalized amplitudes are given by

$$\begin{aligned}
&\mathcal{A}_4^{(1),\mathrm{ren}}(1_t,2,3,4_{\bar{t}}) \\
&= \mathcal{A}_4^{(1)}(1_t,2,3,4_{\bar{t}}) + (\delta Z_G + \delta Z_Q + \delta Z_{g_s})\mathcal{A}_4^{(0)}(1_t,2,3,4_{\bar{t}}) \\
&= \mathcal{A}_4^{(1)}(1_t,2,3,4_{\bar{t}}) - g_s^2 c_\Gamma \mathcal{A}_4^{(0)}(1_t,2,3,4_{\bar{t}}) \\
&\quad \times \left\{ \frac{11N_c - 2N_f}{3\epsilon} - \frac{N_c}{3} + C_F\left(\frac{3}{\epsilon} + 3\log\left(\frac{\mu_R^2}{m^2}\right) + 5\right)\right\},
\end{aligned} \tag{62}$$

$$\begin{aligned}
&\mathcal{A}_4^{(1),\mathrm{ren}}(1_t,2_{\bar{q}},3_q,4_{\bar{t}}) \\
&= \mathcal{A}_4^{(1)}(1_t,2_{\bar{q}},3_q,4_{\bar{t}}) + (\delta Z_Q + \delta Z_{g_s})\mathcal{A}_4^{(0)}(1_t,2_{\bar{q}},3_q,4_{\bar{t}}) \\
&= \mathcal{A}_4^{(1)}(1_t,2_{\bar{q}},3_q,4_{\bar{t}}) - g_s^2 c_\Gamma \mathcal{A}_4^{(0)}(1_t,2_{\bar{q}},3_q,4_{\bar{t}}) \\
&\quad \times \left\{ \frac{11N_c - 2N_f}{3\epsilon} - \frac{N_c}{3} + C_F\left(\frac{3}{\epsilon} + 3\log\left(\frac{\mu_R^2}{m^2}\right) + 5\right)\right. \\
&\quad \left. - \frac{2}{3\epsilon} - \frac{2}{3}\log\left(\frac{\mu_R^2}{m^2}\right)\right\}.
\end{aligned} \tag{63}$$

To convert these renormalized amplitudes to the 't Hooft-Veltman (HV) scheme we follow the well-known universal structure [82–85]. For our amplitudes this can be summarized as

$$\begin{aligned}
&\mathcal{A}_4^{(1),[\mathrm{HV}]}(1_t,2,3,4_{\bar{t}}) \\
&\quad = \mathcal{A}_4^{(1)}(1_t,2,3,4_{\bar{t}}) - g_s^2 c_\Gamma C_F \mathcal{A}_4^{(0)}(1_t,2,3,4_{\bar{t}}),
\end{aligned} \tag{64}$$

$$\begin{aligned}
&\mathcal{A}_4^{(1),[\mathrm{HV}]}(1_t,2_{\bar{q}},3_q,4_{\bar{t}}) \\
&\quad = \mathcal{A}_4^{(1)}(1_t,2_{\bar{q}},3_q,4_{\bar{t}}) - g_s^2 c_\Gamma\left(2C_F - \frac{N_c}{3}\right) \\
&\qquad \times \mathcal{A}_4^{(0)}(1_t,2_{\bar{q}},3_q,4_{\bar{t}}).
\end{aligned} \tag{65}$$

After renormalization, it becomes

$$\begin{aligned}
&\mathcal{A}_4^{(1),[\mathrm{HV}],\mathrm{ren}}(1_t,2,3,4_{\bar{t}}) \\
&\quad = \mathcal{A}_4^{(1),\mathrm{ren}}(1_t,2,3,4_{\bar{t}}) - g_s^2 c_\Gamma \frac{N_c}{3}\mathcal{A}_4^{(0)}(1_t,2,3,4_{\bar{t}}),
\end{aligned} \tag{66}$$

$$\begin{aligned}
&\mathcal{A}_4^{(1),[\mathrm{HV}],\mathrm{ren}}(1_t,2_{\bar{q}},3_q,4_{\bar{t}}) \\
&\quad = \mathcal{A}_4^{(1),\mathrm{ren}}(1_t,2_{\bar{q}},3_q,4_{\bar{t}}) - g_s^2 c_\Gamma C_F \mathcal{A}_4^{(0)}(1_t,2_{\bar{q}},3_q,4_{\bar{t}}).
\end{aligned} \tag{67}$$

VII. TREE LEVEL AMPLITUDES

The tree level amplitudes can be computed using BCFW recursion relations [86,87] together with the spinor conventions of the previous section.

The three-point amplitudes are calculated directly from the Feynman vertex using arbitrary reference vectors. As an example we consider the

$$A_3(1_t^+, 2^{\lambda_2}, 3_{\bar{t}}^+) = \frac{i}{\sqrt{2}}\overline{u_+}(1,m;1^\flat,\eta_1)\not{\epsilon}_{\lambda_2}(2,\xi)v_+(3,m;3,\eta_3), \tag{68}$$

which can be expanded to give

$$A_3(1_t^+, 2^{\lambda_2}, 3_{\bar{t}}^+) = \frac{i}{\sqrt{2}}\frac{\langle\eta_1|(\not{1}+m)\not{\epsilon}_{\lambda_2}(2,\xi)(\not{3}-m)|\eta_3\rangle}{\langle\eta_1 1^\flat\rangle\langle 3^\flat\eta_3\rangle}. \tag{69}$$

The tree level helicity amplitudes, expressed in terms of spinor products, are listed in Appendix A.

VIII. ONE-LOOP AMPLITUDES

In this section we present a complete set of one-loop helicity amplitudes needed for $t\bar{t}$ production at hadron colliders.

A. Notation and integral functions

We define the general scalar integral as[2]

$$I_n = \frac{\mu_R^{2\epsilon}\Gamma(1-2\epsilon)}{i(\pi)^{2-\epsilon}\Gamma(1-\epsilon)^2\Gamma(1+\epsilon)}\int d^D l \frac{1}{\prod_{i=1}^n (l-k_i)^2 - m_i^2}, \tag{70}$$

$\{k_i\}$ are the sums of external momenta entering each of the n vertices of the graph. We will denote the basis integrals for our helicity amplitudes as

$$I_{4;1|2|3|4} = I_4(m^2,0,0,m^2,s_{12},s_{23},m^2,0,0,0) \tag{71}$$

$$I^m_{4;1|2|3|4} = I_4(m^2,0,0,m^2,s_{12},s_{23},0,m^2,m^2,m^2) \tag{72}$$

$$I_{4;1|2|4|3} = I_4(m^2,0,m^2,0,s_{12},s_{13},0,m^2,m^2,0) \tag{73}$$

$$I_{3;12|3|4} = I_3(s_{12},0,m^2,m^2,0,0) \tag{74}$$

$$I^m_{3;12|3|4} = I_3(s_{12},0,m^2,0,m^2,m^2) \tag{75}$$

$$I_{3;13|2|4} = I_3(s_{13},0,m^2,m^2,0,0) \tag{76}$$

$$I^m_{3;13|2|4} = I_3(s_{13},0,m^2,0,m^2,m^2) \tag{77}$$

$$I_{3;2|3|41} = I_3(s_{23},0,0,0,0,0) \tag{78}$$

$$I^m_{3;2|3|41} = I_3(s_{23},0,0,m^2,m^2,m^2) \tag{79}$$

$$I_{3;1|23|4} = I_3(s_{23},m^2,m^2,0,0,m^2) \tag{80}$$

$$I^m_{3;1|23|4} = I_3(s_{23},m^2,m^2,m^2,m^2,0). \tag{81}$$

[2]This follows the conventions of QCDLOOP which was used for numerical evaluations [88].

As described in Sec. IV A 3 we find it convenient to move all $\log(m^2)$ dependence into the on shell bubble. Therefore our helicity amplitudes are written in terms of the following two-point functions:

$$F_{2;12} = I_2(s_{12}, 0, m^2) - I_2(m^2, 0, m^2), \tag{82}$$

$$F^m_{2;23} = I_2(s_{23}, m^2, m^2) - I_2(0, m^2, m^2), \tag{83}$$

$$\hat{I}_{2;23} = I_2(s_{23}, 0, 0) - I_2(m^2, 0, m^2) + 2 + \mathcal{O}(\epsilon), \tag{84}$$

$$I_{2;m} = I_2(m^2, 0, m^2), \tag{85}$$

$$I^m_{2;m} = I_2(0, m^2, m^2), \tag{86}$$

and the tadpole function is removed via

$$I_1(m^2) = m^2(I_2(m^2, 0, m^2) - 1) + \mathcal{O}(\epsilon). \tag{87}$$

Finite box functions are used to make the IR poles explicit:

$$F^m_{4;1|2|3|4} = I^m_{4;1|2|3|4} - \frac{1}{\langle 2|1|2]} I^m_{3;1|23|4}. \tag{88}$$

We also find benefits in cancellation of spurious poles that can be made explicit through the use of higher dimensional integral functions:

$$\begin{aligned} I^{6-2\epsilon}_{4;1|2|3|4} = \frac{1}{2\langle 2|1|3]\langle 3|1|2]} (&-\langle 2|1|2]^2 s_{23} I_{4;1|2|3|4} \\ &+ (\langle 2|1|2] + 2m^2) s_{23} I_{3;1|23|4} + 2\langle 2|1|2]^2 I_{3;12|3|4} \\ &+ \langle 2|1|2] s_{23} I_{3;2|3|41}), \end{aligned} \tag{89}$$

$$\begin{aligned} I^{m,6-2\epsilon}_{4;1|2|3|4} = \frac{1}{2\langle 2|1|3]\langle 3|1|2]} (&-\langle 2|1|2]^2 s_{23} \beta^2 I^m_{4;1|2|3|4} \\ &+ \langle 2|1|2] s_{23} \beta^2 I^m_{3;1|23|4} + 2\langle 2|1|2](\langle 2|1|2] \\ &+ 2m^2) I^m_{3;12|3|4} + s_{23}(\langle 2|1|2] + 2m^2) I^m_{3;2|3|41}). \end{aligned} \tag{90}$$

Since all the expressions are quoted for the same configuration of heavy quark helicities we find it convenient to factor out an overall normalization $\langle \eta_1 1^\flat \rangle \langle \eta_4 4^\flat \rangle$ and define

$$\tilde{A}^{(0)}_4 = -i\langle \eta_1 1^\flat \rangle \langle \eta_4 4^\flat \rangle A^{(0)}_4. \tag{91}$$

B. Primitive amplitudes for $gg \to t\bar{t}$

$$\begin{aligned} &-i\langle \eta_1 1^\flat \rangle \langle \eta_4 4^\flat \rangle A^{[L]}_4(1^+_t, 2^+, 3^+, 4^+_{\bar{t}}) \\ &= I_{4;1|2|3|4}(m^3 \langle \eta_1 \eta_4 \rangle [23]^2) - F_{2;12}\left(\frac{m^3[23](2\langle \eta_1 \eta_4 \rangle s_{12} - \langle \eta_1 | K_{12} K_{23} | \eta_4 \rangle)}{\langle 23 \rangle \langle 2|1|2]^2}\right) + \frac{1}{2}\tilde{A}^{(0)}_4(1^+_t, 2^+, 3^+, 4^+_{\bar{t}}) \times (I_{2;m} - 1) \\ &\quad - \left(\frac{m[23](\langle \eta_1 \eta_4 \rangle \langle 2|1|2] + \langle \eta_1 | K_{12} K_{23} | \eta_4 \rangle)}{2\langle 23 \rangle \langle 2|1|2]} - \frac{m(\langle \eta_1 \eta_4 \rangle \langle 2|1|2] - \langle 2\eta_1 \rangle \langle 3\eta_4 \rangle [23])}{3\langle 23 \rangle^2}\right) \end{aligned} \tag{92}$$

$$\begin{aligned} &i\langle \eta_1 1^\flat \rangle \langle \eta_4 4^\flat \rangle A^{[R]}_4(1^+_t, 2^+, 3^+, 4^+_{\bar{t}}) \\ &= -F^m_{4;1|2|3|4}\left(\frac{\langle 3\eta_1 \rangle \langle 3\eta_4 \rangle [23]^2 m^3 (2m^2 + \langle 2|1|2])}{2\langle 23 \rangle \langle 3|1|2]} - \frac{m^3 \langle 2\eta_1 \rangle \langle 2\eta_4 \rangle [23]^2 (2m^2 + \langle 2|1|2])}{2\langle 23 \rangle \langle 2|1|3]}\right. \\ &\quad \left. + \frac{m^3[23](\langle \eta_1 \eta_4 \rangle (2m^2 - s_{23}) + \langle \eta_1 | K_{12} K_{23} | \eta_4 \rangle)}{\langle 23 \rangle}\right) - I^m_{3;1|23|4}\left(\frac{(2m^2 - s_{23}) \langle \eta_1 \eta_4 \rangle [23] m^3}{\langle 23 \rangle \langle 2|1|2]}\right) \\ &\quad + I^m_{3;12|3|4}\left(\frac{m^3[23](2\langle \eta_1 \eta_4 \rangle \langle 23 \rangle + 4\langle 2\eta_4 \rangle \langle 3\eta_1 \rangle)}{\langle 23 \rangle^2} + \frac{m^3[23] \langle 2\eta_1 \rangle \langle 2\eta_4 \rangle \langle 2|1|2]}{\langle 23 \rangle^2 \langle 2|1|3]}\right. \\ &\quad \left. + \frac{m^3[23](\langle 3\eta_1 \rangle \langle 3\eta_4 \rangle \langle 2|1|3] - \langle 2\eta_1 \rangle \langle 2\eta_4 \rangle \langle 3|1|2])}{\langle 23 \rangle^2 \langle 2|1|2]} - \frac{m^3[23] \langle 3\eta_1 \rangle \langle 3\eta_4 \rangle \langle 2|1|2]}{\langle 23 \rangle^2 \langle 3|1|2]}\right) \\ &\quad - I^m_{3;2|3|41}\left(\frac{m^3 \langle 2\eta_1 \rangle \langle 2\eta_4 \rangle [23]^2}{2\langle 23 \rangle \langle 2|1|3]} - \frac{m^3 \langle 3\eta_1 \rangle \langle 3\eta_4 \rangle [23]^2}{2\langle 23 \rangle \langle 3|1|2]} + \frac{m^3 \langle \eta_1 \eta_4 \rangle [23]}{\langle 23 \rangle}\right) + F_{2;12}\left(\frac{m^3[23](2s_{12}\langle \eta_1 \eta_4 \rangle - \langle \eta_1 | K_{12} K_{23} | \eta_4 \rangle)}{\langle 23 \rangle \langle 2|1|2]^2}\right) \\ &\quad - \frac{1}{2}\tilde{A}^{(0)}_4(1^+_t, 2^+, 3^+, 4^+_{\bar{t}})(I_{2;m} - 1) - \left(\frac{m[23](\langle \eta_1 | K_{12} K_{23} | \eta_4 \rangle + \langle \eta_1 \eta_4 \rangle \langle 2|1|2])}{2\langle 23 \rangle \langle 2|1|2]}\right) \end{aligned} \tag{93}$$

where $K_{ij} = p_i + p_j$.

$$
\begin{aligned}
&- i\langle \eta_1 1^\flat\rangle\langle \eta_4 4^\flat\rangle A_4^{[L]}(1_t^+,2^+,3^-,4_{\bar{t}}^+)\\
&= \tilde{A}_4^{(0)}(1_t^+,2^+,3^-,4_{\bar{t}}^+)\times\left(-s_{23}\langle 2|1|2]I_{4;1|2|3|4}+\frac{1}{2}I_{2;m}-\frac{\langle 2|1|2]+2m^2}{\langle 2|1|2]}F_{2;12}\right)\\
&\quad+\left(I_{3;1|23|4}+\frac{2}{s_{23}}\hat{I}_{2;23}-\frac{4}{s_{23}}\right)\times\left(\frac{3m\langle 3|1|2]\langle\langle 3\eta_1\rangle\langle 3\eta_4\rangle\langle 2|1|3]-\langle 2\eta_1\rangle\langle 2\eta_4\rangle\langle 3|1|2]\rangle}{4\langle 23\rangle\langle 2|1|3]\beta^4}\right)\\
&\quad+\left(I_{3;1|23|4}-\frac{4}{s_{23}}\right)\times\left(\frac{6m^3\langle 2|1|2]\langle 3|1|2]\langle\langle 3\eta_1\rangle\langle 3\eta_4\rangle\langle 2|1|3]-\langle 2\eta_1\rangle\langle 2\eta_4\rangle\langle 3|1|2]\rangle}{\langle 23\rangle\langle 2|1|3]s_{23}^2\beta^4}\right.\\
&\quad\left.-\frac{6m^3\langle 3|1|2]^2(\langle 2\eta_4\rangle\langle 3\eta_1\rangle+\langle 2\eta_1\rangle\langle 3\eta_4\rangle)}{\langle 23\rangle s_{23}^2\beta^4}\right)-\frac{m\langle 3\eta_1\rangle\langle 3\eta_4\rangle\langle 3|1|2][23]}{2}I_{4;1|2|3|4}\\
&\quad+\frac{m\langle 3\eta_1\rangle\langle 3\eta_4\rangle\langle 3|1|2][23]}{2\langle 2|1|2]}I_{3;2|3|41}-\frac{m\langle 3\eta_1\rangle\langle 3\eta_4\rangle\langle 3|1|2]}{\langle 23\rangle}I_{3;12|3|4}+(\hat{I}_{2;23}-2)\frac{m\langle 2\eta_1\rangle\langle 3\eta_4\rangle\langle 3|1|2](2\langle 2|1|2]+s_{23})}{\langle 23\rangle\langle 2|1|3]s_{23}\beta^2}\\
&\quad+I_{4;1|2|3|4}^{6-2\epsilon}\left(\frac{m^3\langle 3\eta_1\rangle\langle 3\eta_4\rangle\langle 3|1|2][23]}{\langle 2|1|2]^2}+\frac{m\langle 2\eta_1\rangle\langle 2\eta_4\rangle\langle 3|1|2](\langle 2|1|2]s_{23}+\langle 2|1|3]\langle 3|1|2])}{\langle 23\rangle\langle 2|1|3]^2}\right.\\
&\quad\left.-\frac{2m^3\langle \eta_1\eta_4\rangle\langle 3|1|2]}{\langle 2|1|3]}+\frac{m\langle \eta_1\eta_4\rangle\langle 3|1|2](\langle 2|1|3]\langle 3|1|2]-\langle 2|1|2]^2)}{\langle 2|1|2]\langle 2|1|3]}+\frac{2m^3\langle 2\eta_1\rangle\langle 3\eta_4\rangle\langle 3|1|2][23]}{\langle 2|1|2]\langle 2|1|3]}\right)\\
&\quad+I_{3;1|23|4}\left(\frac{m\langle 3|1|2]^2(\langle \eta_1\eta_4\rangle\langle 23\rangle+2\langle 2\eta_1\rangle\langle 3\eta_4\rangle)}{\langle 2|1|2]\langle 23\rangle}+\frac{m\langle 2\eta_1\rangle\langle 3\eta_4\rangle\langle 3|1|2](\langle 2|1|2]+2m^2)}{\langle 23\rangle\langle 2|1|3]\beta^2}\right.\\
&\quad-\frac{m\langle 3\eta_1\rangle\langle 3\eta_4\rangle\langle 3|1|2](\langle 2|1|2]^2-\langle 2|1|2]s_{23}+2m^2s_{23})}{2\langle 23\rangle\langle 2|1|2]^2}-\frac{m^3\langle \eta_1\eta_4\rangle\langle 3|1|2]}{\langle 2|1|3]}\\
&\quad+\frac{m\langle 2\eta_1\rangle\langle 3\eta_4\rangle\langle 3|1|2](\langle 2|1|2]+2s_{23})}{\langle 23\rangle\langle 2|1|3]}+\frac{m^3\langle 2\eta_1\rangle\langle 2\eta_4\rangle\langle 3|1|2][23](2\langle 2|1|2]+s_{23})}{\langle 2|1|3]^2s_{23}\beta^2}\\
&\quad\left.+\frac{m\langle 2\eta_1\rangle\langle 2\eta_4\rangle\langle 3|1|2]^2}{2\langle 23\rangle\langle 2|1|3]}-\frac{m\langle 3|1|2][23](\langle 2\eta_1\rangle\langle 2\eta_4\rangle\langle 3|1|2]-\langle 3\eta_1\rangle\langle 3\eta_4\rangle\langle 2|1|3])}{4\langle 2|1|3]s_{23}\beta^2}\right)\\
&\quad+\hat{I}_{2;23}\left(\frac{m\langle 3|1|2](\langle \eta_1\eta_4\rangle\langle 2|1|2]-\langle 2\eta_1\rangle\langle 3\eta_4\rangle[23])}{\langle 2|1|3]s_{23}}-\frac{m\langle 2\eta_1\rangle\langle 2\eta_4\rangle\langle 3|1|2](\langle 2|1|2]+2m^2)}{\langle 23\rangle\langle 2|1|3]^2\beta^2}\right.\\
&\quad-\frac{12m^2+s_{23}\beta^2}{s_{23}\beta^2}\times\frac{m\langle 3|1|2]^2(\langle 2\eta_1\rangle\langle 3\eta_4\rangle+\langle 3\eta_1\rangle\langle 2\eta_4\rangle)}{\langle 23\rangle s_{23}^2\beta^2}\\
&\quad\left.-\frac{12m^2+s_{23}\beta^2}{s_{23}\beta^2}\times\frac{m\langle 2|1|2]\langle 3|1|2](\langle 2\eta_1\rangle\langle 2\eta_4\rangle\langle 3|1|2]-\langle 3\eta_1\rangle\langle 3\eta_4\rangle\langle 2|1|3])}{\langle 23\rangle\langle 2|1|3]s_{23}^2\beta^2}\right)\\
&\quad-F_{2;12}\left(\frac{m\langle \eta_1\eta_4\rangle\langle 3|1|2](\langle 2|1|2]+2m^2)}{\langle 2|1|3]s_{23}}-\frac{m\langle 2\eta_1\rangle\langle 2\eta_4\rangle\langle 2|1|2]\langle 3|1|2]}{\langle 23\rangle\langle 2|1|3]^2}\right.\\
&\quad-\frac{m\langle 3\eta_4\rangle\langle \eta_1|1|2]\langle 3|1|2]}{2\langle 2|1|2]s_{12}}+\frac{m\langle 3\eta_1\rangle\langle 3\eta_4\rangle\langle 3|1|2](2m^2-\langle 2|1|2])}{2\langle 23\rangle\langle 2|1|2]^2}+\frac{2m^3\langle 2\eta_1\rangle\langle 3\eta_4\rangle\langle 3|1|2]}{\langle 23\rangle\langle 2|1|2]\langle 2|1|3]}\\
&\quad\left.+\frac{m\langle 2\eta_1\rangle\langle 3\eta_4\rangle\langle 3|1|2]^2}{\langle 23\rangle\langle 2|1|2]^2}-\frac{m\langle 2\eta_1\rangle\langle 2\eta_4\rangle\langle 3|1|2]^2(2\langle 2|1|2]^2+2\langle 2|1|3]\langle 3|1|2]+\langle 2|1|2]s_{23})}{2\langle 23\rangle\langle 2|1|2]^2\langle 2|1|3]s_{23}}\right)\\
&\quad+\frac{m\langle 3\eta_4\rangle\langle 3|1|2](\langle 2\eta_1\rangle\langle 3|1|2]-\langle 3\eta_1\rangle\langle 2|1|2])}{2\langle 23\rangle\langle 2|1|2]s_{12}}-\frac{2m\langle \eta_1\eta_4\rangle\langle 2|1|2]\langle 3|1|2]}{\langle 2|1|3]s_{23}}\\
&\quad-\frac{m\langle \eta_1\eta_4\rangle\langle 3|1|2]^2}{2\langle 2|1|2]s_{23}}+\frac{m\langle 2\eta_1\rangle\langle 3|1|2](\langle 2\eta_4\rangle\langle 3|1|2]-4\langle 3\eta_4\rangle\langle 2|1|2])}{2\langle 23\rangle\langle 2|1|2]\langle 2|1|3]}-\frac{m\langle 2\eta_1\rangle\langle 2\eta_4\rangle\langle 3|1|2]^2}{\langle 23\rangle\langle 2|1|3]s_{23}\beta^2}\\
&\quad+\frac{m\langle 3\eta_1\rangle\langle 3\eta_4\rangle\langle 3|1|2]}{\langle 23\rangle s_{23}\beta^2}+\frac{2m\langle 2\eta_1\rangle\langle 2\eta_4\rangle\langle 3|1|2](\langle 2|1|2]+2m^2)}{\langle 23\rangle\langle 2|1|3]^2\beta^2}
\end{aligned}
\tag{94}
$$

$$
\begin{aligned}
&i\langle \eta_1 1^\flat\rangle\langle \eta_4 4^\flat\rangle A_4^{[R]}(1_t^+,2^+,3^-,4_{\tilde{t}}^+)\\
&=\tilde{A}_4^{(0)}(1_t^+,2^+,3^-,4_{\tilde{t}}^+)\times\Bigg((s_{23}-2m^2)I^m_{3;1|23|4}-\frac{2m^2(2s_{12}-s_{23})}{\langle 2|1|2]\beta^2}I^m_{3;2|3|41}+\frac{2s_{12}}{\langle 2|1|2]}F_{2;12}-\frac{1}{2}I_{2;m}\Bigg)\\
&\quad+\Bigg(-(\langle 2|1|2]+2m^2)[23]I^{m,6-2\epsilon}_{4;1|2|3|4}+\frac{2m^2\langle 2|1|2]}{\langle 23\rangle}I^m_{3;12|3|4}-m^2[23]I^m_{3;2|3|41}+\frac{\langle 2|1|2]+2m^2}{\langle 23\rangle}F_{2;12}-\frac{\langle 2|1|2]}{\langle 23\rangle}(F^m_{2;23}-2)\Bigg)\\
&\quad\times\frac{m\langle 2\eta_1\rangle\langle 3|1|2](\langle 2\eta_4\rangle\langle 2|1|2]+2\langle 3\eta_4\rangle\langle 2|1|3])}{\langle 2|1|2]\langle 2|1|3]^2}-I^{m,6-2\epsilon}_{4;1|2|3|4}\\
&\quad\times\Bigg(\frac{m^3\langle 2\eta_4\rangle\langle 3\eta_1\rangle\langle 3|1|2]^2}{\langle 23\rangle\langle 2|1|2]^2\beta^2}+\frac{m\langle 3|1|2][23]\langle 3\eta_1\rangle\langle 3\eta_4\rangle(\langle 2|1|2]+2m^2)}{\langle 2|1|2]^2}+\frac{m^3\langle 3\eta_1\rangle\langle 3\eta_4\rangle\langle 3|1|2][23]}{2\langle 2|1|2]^2}\\
&\quad+\frac{m\langle 2\eta_1\rangle\langle 3\eta_4\rangle\langle 3|1|2](2\langle 2|1|2]^2+s_{23}(\langle 2|1|2]+2m^2))}{\langle 23\rangle\langle 2|1|2]\langle 2|1|3]}+\frac{m\langle 2\eta_1\rangle\langle 2\eta_4\rangle\langle 3|1|2]^2(\langle 2|1|2]+2m^2)}{\langle 23\rangle\langle 2|1|3]s_{23}\beta^2}\\
&\quad+\frac{m\langle 2\eta_1\rangle\langle 3|1|2]^2(\langle 2\eta_4\rangle\langle 3|1|2]+\langle 3\eta_4\rangle\langle 2|1|2])}{\langle 23\rangle\langle 2|1|2]s_{23}\beta^2}+\frac{3m\langle 2\eta_1\rangle\langle 3\eta_4\rangle\langle 3|1|2]^2(\langle 2|1|2]^2+s_{12}s_{23})}{\langle 23\rangle\langle 2|1|2]^2s_{23}\beta^2}\\
&\quad+\frac{2m\langle 3\eta_1\rangle\langle 3\eta_4\rangle\langle 3|1|2](\langle 2|1|2]+2m^2)}{\langle 23\rangle\langle 2|1|2]\beta^2}+\frac{m^3\langle 3\eta_1\rangle\langle 3\eta_4\rangle\langle 3|1|2](2\langle 2|1|2]+s_{23})}{2\langle 23\rangle\langle 2|1|2]^2\beta^2}\\
&\quad-\frac{m\langle \eta_1\eta_4\rangle\langle 3|1|2]s_{12}(\langle 2|1|2]^2-s_{12}s_{23})}{\langle 2|1|3]\langle 2|1|2]^2}\Bigg)+F^m_{4;1|2|3|4}\frac{m\langle 3\eta_4\rangle\langle 3|1|2](2\langle 2\eta_1\rangle\langle 3|1|2]+3m^2\langle 3\eta_1\rangle)}{\langle 23\rangle}\\
&\quad+I^m_{3;12|3|4}\Bigg(\frac{5m^3\langle 3\eta_1\rangle\langle 3\eta_4\rangle\langle 3|1|2]}{\langle 23\rangle\langle 2|1|2]}-\frac{2m^3\langle \eta_1\eta_4\rangle\langle 3|1|2]s_{12}}{\langle 2|1|2]\langle 2|1|3]}-\frac{m^3\langle 3\eta_1\rangle\langle 3\eta_4\rangle\langle 3|1|2](8\langle 2|1|2]+s_{23})}{\langle 23\rangle\langle 2|1|2]s_{23}\beta^2}\\
&\quad+\frac{2m^3\langle \eta_1\eta_4\rangle\langle 3|1|2](((\langle 2|1|2]+2m^2)\langle 2|1|2]+\langle 2|1|3]\langle 3|1|2])}{\langle 2|1|2]\langle 2|1|3]s_{23}\beta^2}+\frac{2m^3\langle 2\eta_1\rangle\langle 2\eta_4\rangle\langle 3|1|2]^2}{\langle 23\rangle\langle 2|1|3]s_{23}\beta^2}\\
&\quad-\frac{2m^3\langle 2\eta_1\rangle\langle 3\eta_4\rangle\langle 3|1|2](2\langle 2|1|2]+s_{23})}{\langle 23\rangle\langle 2|1|3]s_{23}\beta^2}-\frac{4m\langle 2\eta_1\rangle\langle 3\eta_4\rangle\langle 3|1|2]^2(\langle 2|1|2]+2m^2)}{\langle 23\rangle\langle 2|1|2]s_{23}\beta^2}\Bigg)\\
&\quad-(F^m_{2;23}-2)\frac{m\langle 3|1|2]^2(\langle 2\eta_4\rangle\langle 3\eta_1\rangle+\langle 2\eta_1\rangle\langle 3\eta_4\rangle)}{\langle 23\rangle s_{23}^2\beta^2}\\
&\quad-I^m_{3;2|3|41}\Bigg(\frac{m\langle 2\eta_1\rangle\langle 3\eta_4\rangle\langle 3|1|2][23]}{\langle 2|1|3]}-\frac{2\langle \eta_1\eta_4\rangle\langle 3|1|2]^2m^3}{\langle 2|1|2]s_{23}\beta^2}\\
&\quad+\frac{2m^3\langle \eta_1\eta_4\rangle\langle 3|1|2](\langle 2|1|2]+2m^2)}{\langle 2|1|3]s_{23}\beta^2}-\frac{6m^5\langle 3\eta_1\rangle\langle 3\eta_4\rangle\langle 3|1|2][23]}{\langle 2|1|2]^2s_{23}\beta^2}\\
&\quad-\frac{m\langle 2\eta_1\rangle\langle 3\eta_4\rangle\langle 3|1|2](2m^2\langle 2|1|2]^2-\langle 2|1|3]\langle 3|1|2](\langle 2|1|2]+4m^2))}{\langle 23\rangle\langle 2|1|2]^2\langle 2|1|3]\beta^2}\\
&\quad-\frac{m\langle 2\eta_1\rangle\langle 3|1|2](\langle 2\eta_4\rangle\langle 3|1|2]s_{12}-\langle \eta_4|1|2]\langle 23\rangle\langle 2|1|2])}{\langle 23\rangle\langle 2|1|2]\langle 2|1|3]\beta^2}\Bigg)\\
&\quad+F_{2;12}\Bigg(\frac{2m\langle \eta_1\eta_4\rangle\langle 3|1|2]s_{12}}{\langle 2|1|3]s_{23}}-\frac{m^3\langle 3\eta_1\rangle\langle 3\eta_4\rangle\langle 3|1|2]}{2\langle 23\rangle\langle 2|1|2]s_{12}}\\
&\quad-\frac{m\langle 2\eta_1\rangle\langle 2\eta_4\rangle\langle 3|1|2]^2}{2\langle 23\rangle\langle 2|1|2]\langle 2|1|3]}-\frac{m\langle 2\eta_1\rangle\langle 3\eta_4\rangle\langle 3|1|2]^2}{2\langle 23\rangle\langle 2|1|2]s_{12}}+\frac{m\langle 2\eta_1\rangle\langle 3\eta_4\rangle\langle 3|1|2]}{\langle 23\rangle\langle 2|1|3]}\Bigg)\\
&\quad-(F^m_{2;23}-2)\times\Bigg(\frac{m\langle \eta_1\eta_4\rangle\langle 2|1|2]\langle 3|1|2]}{\langle 2|1|3]s_{23}}+\frac{m\langle \eta_1\eta_4\rangle\langle 3|1|2](\langle 2|1|2]+2m^2)}{\langle 2|1|3]s_{23}\beta^2}\\
&\quad-\frac{m\langle 3|1|2](2\langle 2|1|2]+3s_{23})(\langle 3\eta_1\rangle\langle 3\eta_4\rangle\langle 2|1|3]-\langle 2\eta_1\rangle\langle 2\eta_4\rangle\langle 3|1|2])}{2\langle 23\rangle\langle 2|1|3]s_{23}^2\beta^2}-\frac{m\langle 2\eta_1\rangle\langle 3\eta_4\rangle\langle 3|1|2](2\langle 2|1|2]+s_{23})}{\langle 23\rangle\langle 2|1|3]s_{23}\beta^2}\Bigg)\\
&\quad+\frac{m\langle 3|1|2]^2(\langle \eta_1\eta_4\rangle\langle 2|1|3]+\langle 2\eta_1\rangle\langle 2\eta_4\rangle[23])}{2\langle 2|1|2]\langle 2|1|3]s_{23}}+\frac{m\langle 3\eta_4\rangle\langle 3|1|2](\langle 3\eta_1\rangle\langle 2|1|2]-\langle 2\eta_1\rangle\langle 3|1|2])}{2\langle 23\rangle\langle 2|1|2]s_{12}}.
\end{aligned}
\tag{95}
$$

The primitive amplitudes contributing to $A_{4;3}$ contain bubble, tadpole and rational terms that cancel when forming the complete amplitude. We do not list these terms explicitly in the following expressions:

$$
\begin{aligned}
&- i\langle\eta_1 1^\flat\rangle\langle\eta_4 4^\flat\rangle A_4^{[L]}(1_t^+, 2^+, 4_{\bar{t}}^+, 3^+) \\
&\quad = +I_{4;1|2|4|3} \times \left(\frac{m^3\langle\eta_1\eta_4\rangle(\langle 3|1|3]^2 - \langle 2|1|2]s_{23})}{\langle 23\rangle^2} - \frac{m^3\langle 3\eta_1\rangle\langle 3\eta_4\rangle[23]\langle 2|1|2]\langle 3|1|3]}{2\langle 23\rangle^2\langle 3|1|2]}\right) \\
&\qquad + (\langle 2|1|2]I_{3;12|3|4} + \langle 3|1|3]I_{3;13|2|4}) \\
&\qquad \times \frac{m^3(2\langle\eta_1\eta_4\rangle\langle 3|1|2] + \langle 3\eta_1\rangle\langle 3\eta_4\rangle[23])}{2\langle 23\rangle^2\langle 3|1|2]} \\
&\qquad + (\langle 2|1|2]I^m_{3;12|3|4} + \langle 3|1|3]I^m_{3;13|2|4}) \\
&\qquad \times \frac{m^3(2\langle\eta_1\eta_4\rangle\langle 3|1|2] - \langle 3\eta_1\rangle\langle 3\eta_4\rangle[23])}{2\langle 23\rangle^2\langle 3|1|2]} \\
&\qquad + (I^m_{3;12|3|4} - I^m_{3;13|2|4}) \times \frac{m^3[23](\langle 2\eta_1\rangle\langle 3\eta_4\rangle + \langle 3\eta_1\rangle\langle 2\eta_4\rangle)}{\langle 23\rangle^2} \\
&\qquad - \left(\frac{I^m_{3;12|3|4}}{\langle 2|1|2]} + \frac{I^m_{3;13|2|4}}{\langle 3|1|3]}\right) \times \frac{m^3\langle 2\eta_1\rangle\langle 2\eta_4\rangle[23]\langle 3|1|2]}{\langle 23\rangle^2} \\
&\qquad + \text{bubbles, tadpoles and rational terms}
\end{aligned}
\tag{96}
$$

$$
\begin{aligned}
&- i\langle\eta_1 1^\flat\rangle\langle\eta_4 4^\flat\rangle A_4^{[L]}(1_t^+, 2^+, 4_{\bar{t}}^+, 3^-) \\
&\quad = +I_{4;1|2|4|3} \times \left(\frac{m(\langle\eta_1\eta_4\rangle\langle 3|1|2] - \langle 3\eta_1\rangle\langle 3\eta_4\rangle[23])(-\langle 2|1|3]\langle 3|1|2] + m^2 s_{23})}{2\langle 2|1|3]}\right. \\
&\qquad + \frac{m^3\langle 2|1|2]\langle 3|1|3](\langle 2\eta_1\rangle\langle 3\eta_4\rangle[23] + \langle\eta_1\eta_4\rangle s_{12})}{\langle 2|1|3]^2} - \frac{3m^3\langle 3\eta_1\rangle\langle 3\eta_4\rangle\langle 2|1|2]\langle 3|1|3]}{2\langle 23\rangle\langle 2|1|3]} \\
&\qquad \left. - \frac{2m^3\langle 2\eta_1\rangle\langle 3\eta_4\rangle\langle 2|1|2]^2\langle 3|1|3]}{\langle 23\rangle\langle 2|1|3]^2} + \frac{m^3\langle 2\eta_1\rangle\langle 2\eta_4\rangle\langle 2|1|2]^2\langle 3|1|3]^2}{2\langle 23\rangle\langle 2|1|3]^3}\right) \\
&\qquad + (I^m_{3;12|3|4} - I_{3;12|3|4})\left(\frac{m^3\langle\eta_1\eta_4\rangle\langle 2|1|2]s_{12}}{\langle 2|1|3]^2} + \frac{m^3\langle 2\eta_1\rangle\langle 2\eta_4\rangle\langle 2|1|2]^2\langle 3|1|3]}{2\langle 23\rangle\langle 2|1|3]^3}\right. \\
&\qquad + \frac{m\langle 2|1|2](\langle\eta_1\eta_4\rangle\langle 3|1|2] - \langle 3\eta_1\rangle\langle 3\eta_4\rangle[23])}{2\langle 2|1|3]} - \frac{3m^3\langle 3\eta_1\rangle\langle 3\eta_4\rangle\langle 2|1|2]}{2\langle 23\rangle\langle 2|1|3]} \\
&\qquad \left. - \frac{m^3\langle 2\eta_1\rangle\langle 3\eta_4\rangle\langle 2|1|2][23]}{\langle 2|1|3]^2} + \frac{2m^3\langle 2\eta_1\rangle\langle 3\eta_4\rangle\langle 2|1|2]\langle 3|1|3]}{\langle 23\rangle\langle 2|1|3]^2}\right) \\
&\qquad + (I^m_{3;13|2|4} - I_{3;13|2|4}) \times \left(\frac{m^3\langle\eta_1\eta_4\rangle\langle 3|1|3]s_{12}}{\langle 2|1|3]^2} + \frac{m^3\langle 2\eta_1\rangle\langle 2\eta_4\rangle\langle 2|1|2]\langle 3|1|3]^2}{2\langle 23\rangle\langle 2|1|3]^3}\right. \\
&\qquad + \frac{m\langle 3|1|3](\langle\eta_1\eta_4\rangle\langle 3|1|2] - \langle 3\eta_1\rangle\langle 3\eta_4\rangle[23])}{2\langle 2|1|3]} \\
&\qquad - \frac{3m^3\langle 3\eta_1\rangle\langle 3\eta_4\rangle\langle 3|1|3]}{2\langle 23\rangle\langle 2|1|3]} + \frac{m^3\langle 2\eta_1\rangle\langle 3\eta_4\rangle\langle 3|1|3][23]}{\langle 2|1|3]^2} \\
&\qquad \left. - \frac{2m^3\langle 2\eta_1\rangle\langle 3\eta_4\rangle\langle 2|1|2]\langle 3|1|3]}{\langle 23\rangle\langle 2|1|3]^2}\right) \\
&\qquad + \text{bubbles, tadpoles and rational terms.}
\end{aligned}
\tag{97}
$$

C. Primitive amplitudes for $q\bar{q} \to t\bar{t}$

$$
\begin{aligned}
&i\langle\eta_1 1^\flat\rangle\langle\eta_4 4^\flat\rangle A_4^{[Ic]}(1_t^+, 2_{\bar{q}}^+, 3_q^-, 4_{\bar{t}}^+) \\
&= \tilde{A}_4^{(0)}(1_t^+, 2_{\bar{q}}^+, 3_q^-, 4_{\bar{t}}^+) \times \Big\{ \frac{s_{23}\langle 2|1|2]}{2} I_{4;1|2|3|4} - \frac{s_{23}}{2} I_{3;2|3|41} + \langle 2|1|2] I_{3;12|3|4} - \Big(s_{23} + \frac{3m^2(2\langle 2|1|2] + s_{23})}{s_{23}\beta^4} \Big) I_{3;1|23|4} \\
&\quad - \frac{8}{3} I_{2;m} + \frac{23}{9} + \frac{12m^2(2\langle 2|1|2] + s_{23})}{s_{23}^2\beta^4} - \Big(\frac{7}{6} + \frac{(2\langle 2|1|2] + s_{23})}{2s_{23}\beta^2} + \frac{6m^2(2\langle 2|1|2] + s_{23})}{s_{23}^2\beta^4} \Big) \hat{I}_{2;23} \Big\} \\
&\quad + \frac{m(\langle 2\eta_1\rangle\langle 2\eta_4\rangle[23] + \langle \eta_1\eta_4\rangle\langle 2|1|3])}{2\langle 2|1|3]^2} \times \Big\{ \langle 2|1|2]^3 I_{4;1|2|3|4} - \langle 2|1|2]^2 I_{3;2|3|41} - \frac{2\langle 2|1|2]^3}{s_{23}} I_{3;12|3|4} \\
&\quad + (s_{12}s_{23} - 2m^2\langle 2|1|2]) I_{3;1|23|4} \Big\} + \Big(I_{3;1|23|4} + \frac{2}{s_{23}}(\hat{I}_{2;23} - 2) \Big) \times \Big(\frac{6m^3(\langle 3\eta_1\rangle\langle 3\eta_4\rangle\langle 2|1|2]^2 + \langle 2\eta_1\rangle\langle 2\eta_4\rangle\langle 3|1|2]^2)}{\langle 23\rangle s_{23}^2\beta^4} \\
&\quad - \frac{6m^3\langle 2\eta_1\rangle\langle 3\eta_4\rangle\langle 3|1|2](2\langle 2|1|2] + s_{23})}{\langle 23\rangle s_{23}^2\beta^4} - \frac{3m^3\langle 3\eta_1\rangle\langle 3\eta_4\rangle}{2\langle 23\rangle\beta^4} \Big) \\
&\quad - (\hat{I}_{2;23} - 2) \times \Big(\frac{m\langle 2\eta_1\rangle\langle 2\eta_4\rangle\langle 3|1|2](\langle 2|1|2] + 2m^2)}{\langle 23\rangle\langle 2|1|3]s_{23}\beta^2} + \frac{2m\langle 2\eta_1\rangle\langle 3\eta_4\rangle\langle 3|1|2]}{\langle 23\rangle s_{23}\beta^2} - \frac{m\langle 3\eta_1\rangle\langle 3\eta_4\rangle s_{12}}{\langle 23\rangle s_{23}\beta^2} \Big) \\
&\quad + I_{3;1|23|4} \Big(\frac{m(\langle 2\eta_1\rangle\langle 2\eta_4\rangle\langle 3|1|2] + \langle 3\eta_1\rangle\langle 3\eta_4\rangle\langle 2|1|3])[23]}{2\langle 2|1|3]} + \frac{m^3\langle 3\eta_1\rangle\langle 3\eta_4\rangle(4\langle 2|1|2] + s_{23})}{2\langle 23\rangle s_{23}\beta^2} \\
&\quad - \frac{m^3\langle 2\eta_1\rangle\langle 2\eta_4\rangle\langle 3|1|2](2\langle 2|1|2] + s_{23})}{\langle 23\rangle\langle 2|1|3]s_{23}\beta^2} - \frac{4m^3\langle 2\eta_1\rangle\langle 3\eta_4\rangle\langle 3|1|2]}{\langle 23\rangle s_{23}\beta^2} \Big) \\
&\quad + \hat{I}_{2;23} \Big(\frac{m(\langle 3\eta_1\rangle\langle 3\eta_4\rangle\langle 2|1|2]^2 + \langle 2\eta_1\rangle\langle 2\eta_4\rangle\langle 3|1|2]^2)}{\langle 23\rangle s_{23}^2\beta^2} - \frac{m\langle 2\eta_1\rangle\langle 3\eta_4\rangle\langle 3|1|2](2\langle 2|1|2] + s_{23})}{\langle 23\rangle s_{23}^2\beta^2} - \frac{m^3\langle 3\eta_1\rangle\langle 3\eta_4\rangle}{\langle 23\rangle s_{23}\beta^2} \Big) \\
&\quad + F_{2;12} \Big(\frac{m\langle 2\eta_1\rangle\langle 2\eta_4\rangle\langle 3|1|2]^2}{s_{23}\langle 23\rangle\langle 2|1|2]} + \frac{m\langle 2\eta_1\rangle\langle 2\eta_4\rangle\langle 2|1|2]\langle 3|1|2]}{s_{23}\langle 23\rangle\langle 2|1|3]} - \frac{m\langle 3\eta_4\rangle(\langle 2\eta_1\rangle\langle 3|1|2] + m^2\langle 3\eta_1\rangle)}{\langle 23\rangle\langle 2|1|2]} \Big)
\end{aligned} \tag{98}
$$

$$
\begin{aligned}
-i\langle\eta_1 1^\flat\rangle\langle\eta_4 4^\flat\rangle A_4^{[slc]}(1_t^+, 2_{\bar{q}}^+, 3_q^-, 4_{\bar{t}}^+) &= -\tilde{A}_4^{(0)}(1_t^+, 2_{\bar{q}}^+, 3_q^-, 4_{\bar{t}}^+) \times \Big(s_{23} I_{3;2|3|41} + (s_{23} - 2m^2) I_{3;1|23|4}^m + \frac{3}{2}\hat{I}_{2;23} \\
&\quad + \Big(1 + \frac{2\langle 2|1|2] + s_{23}}{2s_{23}\beta^2} \Big) F_{2;23}^m + I_{2;m} - 4 - \frac{2\langle 2|1|2] + s_{23}}{s_{23}\beta^2} \Big) \\
&\quad - (F_{2;23}^m - 2) \times \Big(\frac{m^3\langle 3\eta_1\rangle\langle 3\eta_4\rangle}{\langle 23\rangle s_{23}\beta^2} + \frac{m\langle 2\eta_1\rangle\langle 3\eta_4\rangle\langle 3|1|2](2\langle 2|1|2] + s_{23})}{\langle 23\rangle s_{23}^2\beta^2} \\
&\quad - \frac{m(\langle 3\eta_1\rangle\langle 3\eta_4\rangle\langle 2|1|2]^2 + \langle 2\eta_1\rangle\langle 2\eta_4\rangle\langle 3|1|2]^2)}{\langle 23\rangle s_{23}^2\beta^2} \Big).
\end{aligned} \tag{99}
$$

D. Fermion loop amplitudes

Below we list the heavy fermion loop corrections for an arbitrary mass m_H. The light fermion loop contributions can be obtained by taking $m_H \to 0$:

$$
\begin{aligned}
&-i\langle\eta_1 1^\flat\rangle\langle\eta_4 4^\flat\rangle A_4^{[H]}(1_t^+, 2^+, 3^+, 4_{\bar{t}}^+) \\
&\quad = -\frac{2m(\langle\eta_1\eta_4\rangle\langle 2|1|2] - \langle 2\eta_1\rangle\langle 3\eta_4\rangle[23])}{\langle 23\rangle^3[23]} \\
&\qquad \times \Big(s_{23} m_H^2 I_{3;2|3|41}^{m_H} + 2m_H^2 F_{2;23}^{m_H} + \frac{1}{6} s_{23} \Big),
\end{aligned} \tag{100}
$$

$$
-iA_4^{[H]}(1_t^+, 2^+, 3^-, 4_{\bar{t}}^+) = 0, \tag{101}
$$

$$
\begin{aligned}
-iA^{[H]}(1_t^+, 2_{\bar{q}}^+, 3_q^-, 4_{\bar{t}}^+) &= -\frac{2i}{3} A_4^{(0)}(1_t^+, 2_{\bar{q}}^+, 3_q^-, 4_{\bar{t}}^+) \\
&\quad \times \Big(\Big(2\frac{m_H^2}{s_{23}} + 1 \Big) F_{2;23}^{m_H} + I_{2;m}^{m_H} - \frac{1}{3} \Big).
\end{aligned} \tag{102}
$$

IX. NUMERICAL RESULTS

The amplitudes in the previous section have been implemented into an efficient library for evaluation of the color and helicity summed interference with tree level. In

order to minimize the number of independent spinor products a specific choice of $\eta_1 = \eta_4 = p_2$ was made. This raises a number of issues since the symmetries between the helicity amplitudes are broken, however it is straightforward to generate all the necessary configurations automatically from those presented here.

For illustrative purposes we present numerical values for the unrenormalized amplitudes in the FDH scheme with the strong coupling set to one. We choose a generic phase-space point for the momenta as follows:

$$p_1 = (-\sqrt{s+m^2}, \sqrt{s}, 0, 0), \tag{103}$$

$$p_2 = \sqrt{s+m^2}(1, \sin\theta, \cos\theta\cos\phi, \cos\theta\sin\phi), \tag{104}$$

$$p_2 = \sqrt{s+m^2}(1, -\sin\theta, -\cos\theta\cos\phi, -\cos\theta\sin\phi), \tag{105}$$

$$p_4 = (-\sqrt{s+m^2}, -\sqrt{s}, 0, 0). \tag{106}$$

The mass of the heavy quark is $m = 1.75$. Numerical results at the point $s = 1$, $\theta = \frac{\pi}{3}$, $\phi = \frac{\pi}{4}$, $N_f = 5$, $N_H = 1$, $N_c = 3$ are given in Table I. The interference with the tree level amplitude summed over helicity and color is given in Table II at two values of the renormalization scale, $\mu_R^2 = m^2$ and $\mu_R^2 = 4m^2$.

Our results have been cross-checked against previous calculations in the literature. At the amplitude level we find full agreement with numerical results of [19].[3] We have also checked against the analytic results of Ref. [16] up to $\mathcal{O}(\epsilon^0)$. We find full agreement with the implementation of the results of Ref. [46] into MCFM [47].

The FORTRAN program used to generate the results of Table II evaluates the interference of one-loop amplitudes with the tree level, summed over helicity and color, in 43 μs for the gluon fusion channel and 13 μs for the quark annihilation channel. Roughly 60% of this time is spent on the evaluation of the scalar integrals. The code was compiled using GFORTRAN with optimization level -O2 and evaluated on a 2.93 GHZ Intel Core i3 530 CPU. The FORTRAN code BSYPPTT and the FORM files used to produce it are available from http://www.nbia.dk/badger.html. Both color and helicity summed results and the individual primitive amplitudes are included.

TABLE I. Numerical values for the individual primitive amplitudes. The reference vectors are chosen as $\eta_1 = (3, 2, 2, 1)$ and $\eta_4 = (3, 2, 1, 2)$, $\mu_R = 2m$.

Primitive Amplitude	ϵ^0
$A_4^{(0)}(1_t^+, 2^+, 3^+, 4_{\bar{t}}^+)$	$0.055220794 + 0.014807839i$
$A_4^{(0)}(1_t^+, 2^+, 3^-, 4_{\bar{t}}^+)$	$0.062949503 + 0.14075936i$
$A_4^{[L]}(1_t^+, 2^+, 3^+, 4_{\bar{t}}^+)$	$0.50453481 + 0.3385402i$
$A_4^{[R]}(1_t^+, 2^+, 3^+, 4_{\bar{t}}^+)$	$0.021100789 - 0.12891563i$
$A_4^{[H]}(1_t^+, 2^+, 3^+, 4_{\bar{t}}^+)$	$-0.01309239 + 0.028932428i$
$A_4^{[f]}(1_t^+, 2^+, 3^+, 4_{\bar{t}}^+)$	$-0.0039170375 - 0.04534929i$
$A_{4;3}(1_t^+, 2^+, 3^+, 4_{\bar{t}}^+)$	$0.63758829 - 1.1392369i$
$A_4^{[L]}(1_t^+, 2^+, 3^-, 4_{\bar{t}}^+)$	$1.1550236 + 1.3088169i$
$A_4^{[R]}(1_t^+, 2^+, 3^-, 4_{\bar{t}}^+)$	$2.5565516 + 1.0995254i$
$A_4^{[H]}(1_t^+, 2^+, 3^-, 4_{\bar{t}}^+)$	0
$A_4^{[f]}(1_t^+, 2^+, 3^-, 4_{\bar{t}}^+)$	0
$A_{4;3}(1_t^+, 2^+, 3^-, 4_{\bar{t}}^+)$	$11.18323 - 1.475571i$
$A_4^{(0)}(1_t^+, 2_{\bar{q}}^+, 3_q^-, 4_{\bar{t}}^+)$	$0.85072714 + 0.25682619i$
$A_4^{[lc]}(1_t^+, 2_{\bar{q}}^+, 3_q^-, 4_{\bar{t}}^+)$	$8.0971525 + 3.2796876i$
$A_4^{[slc]}(1_t^+, 2_{\bar{q}}^+, 3_q^-, 4_{\bar{t}}^+)$	$15.65914 - 4.9530347i$
$A_4^{[H]}(1_t^+, 2_{\bar{q}}^+, 3_q^-, 4_{\bar{t}}^+)$	$1.3699007 + 1.7416922i$
$A_4^{[f]}(1_t^+, 2_{\bar{q}}^+, 3_q^-, 4_{\bar{t}}^+)$	$0.24709861 + 2.0187408i$

X. CONCLUSIONS

In this paper we have used the newly developed techniques of generalized unitarity to compute compact analytic representations of all helicity amplitudes relevant for heavy quark production at hadron colliders. Compact tree level input was generated via BCFW recursion relations and the coefficients of the scalar integral computed via a purely algebraic procedure. A fully automated Feynman diagram approach was used to produce compact forms for the tadpole and rational terms.

The calculation was performed in the spinor-helicity formalism with a completely general representation for the heavy quark spinors. The final amplitudes are expressed in terms of a relatively small set of spinor products. The analytic forms of the helicity amplitudes allow us to take a new look at the structure of the one-loop helicity amplitudes. The all-plus helicity configuration in the gluon channel takes a remarkably simple structure. In comparison to the well-known MHV structure in massless amplitudes it is expected that such a simplicity persists at higher multiplicity. The most notable feature of this new representation is the cancellation of bubbles and rational terms in the subleading color contribution to $gg \to t\bar{t}$, which is expected to be related to the stronger UV constraints on this sector. Together with similar features found in other analytic computations [64], this may motivate future investigations.

The final results yield a flexible implementation suitable for computations of spin correlations and decays in the narrow width approximation.

We have demonstrated that such techniques provide a feasible method to calculate analytic one-loop amplitudes with full mass dependence and serve as a solid base for future implementations of higher multiplicity amplitudes.

[3] A description of the reference vectors used to verify the results of Ref. [19] is given in Appendix B.

TABLE II. Numerical values for the interference between virtual and tree level amplitudes summed over helicity and color, $2\sum_{c,h}\mathcal{A}_4^{(1)}[\mathcal{A}_4^{(0)}]^*$.

Channel	$\frac{1}{\epsilon^2}$	$\frac{1}{\epsilon}$	ϵ^0
$gg \to t\bar{t}(\mu_R = m)$	-882.7183832	$1406.029038 - 1915.339983i$	$2811.35321 + 1478.791625i$
$gg \to t\bar{t}(\mu_R = 2m)$	-882.7183832	$182.3215209 - 1915.339983i$	$3912.313922 - 1176.433394i$
$q\bar{q} \to t\bar{t}(\mu_R = m)$	-82.70769231	$313.1028325 + 73.26833668i$	$152.9616128 - 326.7068046i$
$q\bar{q} \to t\bar{t}(\mu_R = 2m)$	-82.70769231	$198.4456251 + 73.26833668i$	$507.5399839 - 225.1353226i$

ACKNOWLEDGMENTS

We are particularly grateful to Keith Ellis, John Campbell, Peter Uwer and Sven-Olaf Moch for helpful discussions and feedback throughout this project. The work of V. Y. was supported by DFG Contract No. SFB-TR-9 and by LHCPhenoNet network Contract No. PITN-GA-2010-264564. The work of S. B. has been supported in part by Danish Natural Science Research Council Grant No. 10-084954. The work of R. S. was supported in part by Grant No. GK 1504 of the DFG Graduiertenkolleg.

APPENDIX A: TREE LEVEL AMPLITUDES

For completeness we present the tree level amplitudes relevant for our computation using the spinor-helicity formalism described in Sec. III.

1. On shell three-point vertices

The independent on shell three-point vertices are

$$-iA_3(1_t^+, 2^+, 3_{\bar{t}}^+) = \frac{\langle\xi|1|2]}{\langle\xi 2\rangle}\frac{m\langle\eta_1\eta_3\rangle}{\langle\eta_1 1^\flat\rangle\langle\eta_3 3^\flat\rangle}, \tag{A1}$$

$$-iA_3(1_t^-, 2^+, 3_{\bar{t}}^-) = \frac{\langle\xi|1|2]}{\langle\xi 2\rangle}\frac{\langle 1^\flat 3^\flat\rangle}{m}, \tag{A2}$$

$$-iA_3(1_t^-, 2^+, 3_{\bar{t}}^+) = -\frac{\langle\xi|1|2]}{\langle\xi 2\rangle}\frac{\langle 1^\flat\eta_3\rangle}{\langle 3^\flat\eta_1\rangle}, \tag{A3}$$

$$-iA_3(1_t^+, 2^+, 3_{\bar{t}}^-) = \frac{\langle\xi|1|2]}{\langle\xi 2\rangle}\frac{\langle 3^\flat\eta_1\rangle}{\langle 1^\flat\eta_3\rangle}. \tag{A4}$$

2. $gg \to t\bar{t}$ Tree amplitudes

For the $gg \to \bar{t}t$ channel with adjacent fermions we obtain

$$-iA_4^{(0)}(1_t^+, 2^+, 3^+, 4_{\bar{t}}^+) = \frac{m^3\langle\eta_1\eta_4\rangle[23]}{\langle 23\rangle\langle 2|1|2]\langle\eta_1 1^\flat\rangle\langle\eta_4 4^\flat\rangle}, \tag{A5}$$

$$-iA_4^{(0)}(1_t^+, 2^+, 3^-, 4_{\bar{t}}^+) = \frac{m\langle 3|1|2]\big(\langle\eta_1\eta_4\rangle\langle 3|1|2] - [23]\langle 3\eta_1\rangle\langle 3\eta_4\rangle\big)}{s_{23}\langle 2|1|2]\langle\eta_1 1^\flat\rangle\langle\eta_4 4^\flat\rangle}. \tag{A6}$$

For the subleading color contributions we also make use of compact forms for the case of nonadjacent fermions:

$$-iA_4^{(0)}(1_t^+, 2^+, 4_{\bar{t}}^+, 3^+) = \frac{m^3\langle\eta_1\eta_4\rangle[23]^2}{\langle\eta_1 1^\flat\rangle\langle\eta_4 4^\flat\rangle\langle 2|1|2]\langle 3|1|3]}, \tag{A7}$$

$$-iA_4^{(0)}(1_t^+, 2^+, 4_{\bar{t}}^+, 3^-) = -\frac{m\langle 3|1|2]\big(\langle\eta_1\eta_4\rangle\langle 3|1|2] - [23]\langle 3\eta_1\rangle\langle 3\eta_4\rangle\big)}{\langle\eta_1 1^\flat\rangle\langle\eta_4 4^\flat\rangle\langle 2|1|2]\langle 3|1|3]}. \tag{A8}$$

The other fermion helicity states can be obtained via the relation given in (23).

3. $q\bar{q} \to t\bar{t}$ Tree amplitudes

There is only one independent helicity amplitude in this channel which can be written as

$$-iA_4^{(0)}(1_t^+, 2_{\bar{q}}^+, 3_q^-, 4_{\bar{t}}^+) = \frac{m\big(\langle\eta_1 3\rangle\langle\eta_4|4|2] + \langle\eta_4 3\rangle\langle\eta_1|1|2]\big)}{\langle\eta_1 1^\flat\rangle\langle\eta_1 4^\flat\rangle s_{23}}. \tag{A9}$$

APPENDIX B: CONVERSION TO FOUR COMPONENT DIRAC SPINORS

We note that the formalism of Eqs. (19) and (20) can be connected with a more conventional approach to massive solutions of the Dirac equation by choosing a specific reference frame. For a massive four-vector $Q^\mu = (E, Q_1, Q_2, Q_3)$ with $Q^2 = m^2$ we first define

$$Q_+ = E + Q_3, \qquad Q_- = E - Q_3, \tag{B1}$$

$$Q^\perp = Q_1 + iQ_2, \qquad \bar{Q}^\perp = Q_1 - iQ_2. \tag{B2}$$

Making a choice of

$$\eta = \frac{1}{2(Q_- + m)^2}\begin{pmatrix} (Q_- + m)^2 + Q_1^2 + Q_2^2 \\ 2Q_1(Q_- + m) \\ 2Q_2(Q_- + m) \\ -(Q_- + m)^2 + Q_1^2 + Q_2^2 \end{pmatrix}, \tag{B3}$$

then yields the following four dimensional representations:

$$u_+(Q,m)=\begin{pmatrix}\sqrt{E+m}\\ 0\\ \frac{Q_3}{\sqrt{E+m}}\\ \frac{Q^\perp}{\sqrt{E+m}}\end{pmatrix},\qquad u_-(Q,m)=\begin{pmatrix}0\\ \sqrt{E+m}\\ \frac{\bar{Q}^\perp}{\sqrt{E+m}}\\ -\frac{Q_3}{\sqrt{E+m}}\end{pmatrix}, \tag{B4}$$

$$v_+(Q,m)=\begin{pmatrix}\frac{Q_3}{\sqrt{E+m}}\\ \frac{Q^\perp}{\sqrt{E+m}}\\ \sqrt{E+m}\\ 0\end{pmatrix},\qquad v_-(Q,m)=\begin{pmatrix}\frac{\bar{Q}^\perp}{\sqrt{E+m}}\\ -\frac{Q_3}{\sqrt{E+m}}\\ 0\\ \sqrt{E+m}\end{pmatrix}. \tag{B5}$$

This allows a simple way to compare analytic results with numerical ones in the literature.

[1] W. Bernreuther, J. Phys. G **35**, 083001 (2008).
[2] P. Nason, S. Dawson, and R. K. Ellis, Nucl. Phys. **B303**, 607 (1988).
[3] P. Nason, S. Dawson, and R. K. Ellis, Nucl. Phys. **B327**, 49 (1989).
[4] W. Beenakker, H. Kuijf, W. L. van Neerven, and J. Smith, Phys. Rev. D **40**, 54 (1989).
[5] S. Frixione, M. L. Mangano, P. Nason, and G. Ridolfi, Phys. Lett. B **351**, 555 (1995).
[6] W. Bernreuther, A. Brandenburg, Z. G. Si, and P. Uwer, Nucl. Phys. **B690**, 81 (2004).
[7] K. Melnikov and M. Schulze, J. High Energy Phys. 08 (2009) 049.
[8] W. Beenakker *et al.*, Nucl. Phys. **B411**, 343 (1994).
[9] W. Bernreuther, M. Fücker, and Z. Si, Phys. Lett. B **633**, 54 (2006).
[10] J. H. Kühn, A. Scharf, and P. Uwer, Eur. Phys. J. C **45**, 139 (2006).
[11] S. Moretti, M. R. Nolten, and D. A. Ross, Phys. Lett. B **639**, 513 (2006).
[12] W. Bernreuther, M. Fücker, and Z.-G. Si, Phys. Rev. D **74**, 113005 (2006).
[13] J. H. Kühn, A. Scharf, and P. Uwer, Eur. Phys. J. C **51**, 37 (2007).
[14] W. Hollik and M. Kollar, Phys. Rev. D **77**, 014008 (2008).
[15] J. G. Körner, Z. Merebashvili, and M. Rogal, Phys. Rev. D **73**, 034030 (2006).
[16] C. Anastasiou and S. M. Aybat, Phys. Rev. D **78**, 114006 (2008).
[17] S. Dittmaier, P. Uwer, and S. Weinzierl, Phys. Rev. Lett. **98**, 262002 (2007).
[18] S. Dittmaier, P. Uwer, and S. Weinzierl, Eur. Phys. J. C **59**, 625 (2008).
[19] R. K. Ellis, W. T. Giele, Z. Kunszt, and K. Melnikov, Nucl. Phys. **B822**, 270 (2009).
[20] K. Melnikov and M. Schulze, Nucl. Phys. **B840**, 129 (2010).
[21] A. Bredenstein, A. Denner, S. Dittmaier, and S. Pozzorini, J. High Energy Phys. 08 (2008) 108.
[22] A. Bredenstein, A. Denner, S. Dittmaier, and S. Pozzorini, Phys. Rev. Lett. **103**, 012002 (2009).
[23] A. Bredenstein, A. Denner, S. Dittmaier, and S. Pozzorini, J. High Energy Phys. 03 (2010) 021.
[24] G. Bevilacqua, M. Czakon, C. Papadopoulos, R. Pittau, and M. Worek, J. High Energy Phys. 09 (2009) 109.
[25] G. Bevilacqua, M. Czakon, C. G. Papadopoulos, and M. Worek, Phys. Rev. Lett. **104**, 162002 (2010).
[26] A. Denner, S. Dittmaier, S. Kallweit, and S. Pozzorini, arXiv:1012.3975.
[27] G. Bevilacqua, M. Czakon, A. van Hameren, C. G. Papadopoulos, and M. Worek, arXiv:1012.4230.
[28] Z. Bern, L. J. Dixon, D. C. Dunbar, and D. A. Kosower, Nucl. Phys. **B425**, 217 (1994).
[29] Z. Bern, L. J. Dixon, D. C. Dunbar, and D. A. Kosower, Nucl. Phys. **B435**, 59 (1995).
[30] C. F. Berger *et al.*, Phys. Rev. D **78**, 036003 (2008).
[31] R. K. Ellis, W. T. Giele, and Z. Kunszt, J. High Energy Phys. 03 (2008) 003.
[32] W. T. Giele, Z. Kunszt, and K. Melnikov, J. High Energy Phys. 04 (2008) 049.
[33] G. Ossola, C. G. Papadopoulos, and R. Pittau, Nucl. Phys. **B763**, 147 (2007).
[34] W. Giele and G. Zanderighi, J. High Energy Phys. 06 (2008) 038.
[35] P. Mastrolia, G. Ossola, T. Reiter, and F. Tramontano, J. High Energy Phys. 08 (2010) 080.
[36] G. Ossola, C. G. Papadopoulos, and R. Pittau, J. High Energy Phys. 03 (2008) 042.
[37] S. Badger, B. Biedermann, and P. Uwer, arXiv:1011.2900.
[38] R. K. Ellis, K. Melnikov, and G. Zanderighi, J. High Energy Phys. 04 (2009) 077.
[39] R. K. Ellis, K. Melnikov, and G. Zanderighi, Phys. Rev. D **80**, 094002 (2009).
[40] C. F. Berger *et al.*, Phys. Rev. Lett. **102**, 222001 (2009).
[41] C. F. Berger *et al.*, Phys. Rev. D **80**, 074036 (2009).
[42] C. F. Berger *et al.*, Phys. Rev. D **82**, 074002 (2010).
[43] T. Melia, K. Melnikov, R. Rontsch, and G. Zanderighi, J. High Energy Phys. 12 (2010) 053.
[44] C. F. Berger *et al.*, arXiv:1009.2338.
[45] R. Frederix, S. Frixione, K. Melnikov, and G. Zanderighi, J. High Energy Phys. 11 (2010) 050.
[46] J. G. Körner and Z. Merebashvili, Phys. Rev. D **66**, 054023 (2002).
[47] R. K. Ellis and J. Campbell, http://mcfm.fnal.gov.
[48] Z. Bern, L. J. Dixon, and D. A. Kosower, Nucl. Phys. **B437**, 259 (1995).
[49] R. Kleiss and W. J. Stirling, Nucl. Phys. **B262**, 235 (1985).

[50] C. Schwinn and S. Weinzierl, J. High Energy Phys. 05 (2005) 006.
[51] G. Rodrigo, J. High Energy Phys. 09 (2005) 079.
[52] K. Hagiwara and D. Zeppenfeld, Nucl. Phys. **B274**, 1 (1986).
[53] D. Maitre and P. Mastrolia, Comput. Phys. Commun. **179**, 501 (2008).
[54] C. Anastasiou, R. Britto, B. Feng, Z. Kunszt, and P. Mastrolia, Phys. Lett. B **645**, 213 (2007).
[55] C. Anastasiou, R. Britto, B. Feng, Z. Kunszt, and P. Mastrolia, J. High Energy Phys. 03 (2007) 111.
[56] R. Britto, F. Cachazo, and B. Feng, Nucl. Phys. **B725**, 275 (2005).
[57] D. Forde, Phys. Rev. D **75**, 125019 (2007).
[58] P. Mastrolia, Phys. Lett. B **678**, 246 (2009).
[59] Z. Bern and A. G. Morgan, Nucl. Phys. **B467**, 479 (1996).
[60] S. D. Badger, Nucl. Phys. B, Proc. Suppl. **183**, 220 (2008).
[61] R. Britto and B. Feng, Phys. Rev. D **75**, 105006 (2007).
[62] W. B. Kilgore, arXiv:0711.5015.
[63] L. J. Dixon and Y. Sofianatos, J. High Energy Phys. 08 (2009) 058.
[64] S. Badger, E. W. Nigel Glover, P. Mastrolia, and C. Williams, J. High Energy Phys. 01 (2010) 036.
[65] S. Badger, J. M. Campbell, R. K. Ellis, and C. Williams, J. High Energy Phys. 12 (2009) 035.
[66] S. Badger, J. M. Campbell, and R. K. Ellis, arXiv:1011.6647.
[67] R. Britto, arXiv:1012.4493.
[68] C. F. Berger and D. Forde, Annu. Rev. Nucl. Part. Sci. **60**, 181 (2010).
[69] R. Britto, B. Feng, and P. Mastrolia, Phys. Rev. D **78**, 025031 (2008).
[70] S. D. Badger, J. High Energy Phys. 01 (2009) 049.
[71] Z. Bern, L. J. Dixon, and D. A. Kosower, Phys. Rev. D **71**, 105013 (2005).
[72] Z. Bern, L. J. Dixon, and D. A. Kosower, Phys. Rev. D **72**, 125003 (2005).
[73] Z. Bern, L. J. Dixon, and D. A. Kosower, Phys. Rev. D **73**, 065013 (2006).
[74] C. F. Berger, Z. Bern, L. J. Dixon, D. Forde, and D. A. Kosower, Phys. Rev. D **74**, 036009 (2006).
[75] R. Britto and B. Feng, Phys. Lett. B **681**, 376 (2009).
[76] R. Britto and E. Mirabella, arXiv:1011.2344.
[77] M. Tentyukov and J. Fleischer, Comput. Phys. Commun. **132**, 124 (2000).
[78] J. A. M. Vermaseren, arXiv:math-ph/0010025.
[79] A. I. Davydychev, Phys. Lett. B **263**, 107 (1991).
[80] J. Fleischer, F. Jegerlehner, and O. V. Tarasov, Nucl. Phys. **B566**, 423 (2000).
[81] T. Diakonidis, J. Fleischer, T. Riemann, and J. Tausk, Phys. Lett. B **683**, 69 (2010).
[82] J. Fleischer and T. Riemann, arXiv:1009.4436.
[83] S. Catani, S. Dittmaier, and Z. Trócsányi, Phys. Lett. B **500**, 149 (2001).
[84] W. Beenakker *et al.*, Nucl. Phys. **B653**, 151 (2003).
[85] B. W. Harris, E. Laenen, L. Phaf, Z. Sullivan, and S. Weinzierl, Phys. Rev. D **66**, 054024 (2002).
[86] Z. Kunszt, A. Signer, and Z. Trócsányi, Nucl. Phys. **B411**, 397 (1994).
[87] R. Britto, F. Cachazo, and B. Feng, Nucl. Phys. **B715**, 499 (2005).
[88] R. Britto, F. Cachazo, B. Feng, and E. Witten, Phys. Rev. Lett. **94**, 181602 (2005).
[89] R. K. Ellis and G. Zanderighi, J. High Energy Phys. 02 (2008) 002.